

**EXPERIMENTAL INVESTIGATION ON RHEOLOGY AND  
STRENGTH OF BLAST FURNACE SLAG-FLY ASH BASED  
ALKALI ACTIVATED BINDER SYSTEMS WITH  
ADMIXTURES**

PROJECT REPORT

Submitted by

**ASWANI V**

**REG NO.: TKM20CESC06**

**ROLL NO.: M20CESC05**

To

the A P J Abdul Kalam Technological University

in partial fulfillment of the requirements for the award of the Degree of

Master of Technology in

*Structural Engineering & Construction Management*



**Department of Civil Engineering**

**TKM College of Engineering, Kollam-691005**

**SEP 2022**

## **DECLARATION**

I undersigned hereby declare that the project report “Experimental investigation on rheology and strength of blast furnace slag-fly ash based alkali activated binder systems with admixtures”, submitted for partial fulfilment of the requirements for the award of the degree of Master of Technology of the APJ Abdul Kalam Technological University, Kerala, is a bonafide work done by me under supervision of Dr. Ramaswamy K. P., Assistant Professor, Department of civil engineering, TKM College of Engineering. This submission represents my ideas in my own words and where ideas or words of others have been included. I have adequately and accurately cited and referenced the original sources. I also declare that I have adhered to ethics of academic honesty and integrity and have not misrepresented or fabricated any data or idea or fact or source in my submission. I understand that any violation of the above will be a cause for disciplinary action by the institute and/or the University and can also evoke penal action from the sources which have thus not been properly cited or from whom proper permission has not been obtained. This report has not previously formed the basis for the award of any degree, diploma or similar title of any other University.

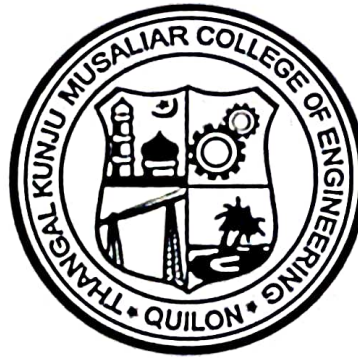
Kollam

Aswani V

12/09/2022

**DEPARTMENT OF CIVIL ENGINEERING**

**T.K.M. College of Engineering, Kollam**



**CERTIFICATE**

Certified that this report entitled '**EXPERIMENTAL INVESTIGATION ON RHEOLOGY AND STRENGTH OF BLAST FURNACE SLAG-FLY ASH BASED ALKALI ACTIVATED BINDER SYSTEMS WITH ADMIXTURES**' is the report of the project presented by **ASWANI V**, Roll No: **TKM20CESC06** during **2021-2022** in partial fulfilment of the requirements for the award of the Degree of Master of Technology in Structural Engineering & Construction Management of the A P J AbdulKalam Technological University.

*Guide*

*Coordinator*

*Head of the Department*

**Dr. RAMASWAMY K.P.**

Assistant Professor,  
Department of  
Civil Engineering.

**Dr. RAMASWAMY K.P.**

Assistant Professor,  
Department of  
Civil Engineering.

**Dr. SAJEEB R.**

Professor,  
Department of  
Civil Engineering.

## **ACKNOWLEDGEMENT**

I take this opportunity to express my deep sense of gratitude and sincere thanks to all who helped me to complete the project successfully.

I would like to convey my heartfelt gratitude to my guide and project coordinator, Dr. Ramaswamy K. P., Assistant Professor, Department of Civil Engineering, TKM College of Engineering, for his excellent guidance, positive criticism and invaluable advice given at every stage of my M. Tech thesis work.

I would also like to express my grateful acknowledgement to Ms. Shobha Elizabeth Thomas, Research Scholar, Department of Civil Engineering, TKM College of Engineering for her precious assistance and valuable comments throughout the completion of this project.

I am greatly thankful to Dr. Sajeeb R., Professor and Head of the Department, Department of Civil Engineering, TKM College of Engineering, for his kind support.

Finally, I wish to express my sincere thanks to my friends for their kind suggestions, encouragements and intangible support for my project work.

Aswani V

## ABSTRACT

Alkali activated binders (AABs) are a sustainable alternative to Portland cement. They make use of industrial byproducts rich in aluminosilicates to produce hardened binder which contain contains hydrous alkali-aluminosilicates under alkaline condition. The local availability of suitable raw materials (precursors and activators) is a key factor to determine the utilization of alkali-activated binders in any specific location. This study thus focuses on using locally available industrial byproducts to make AABs. Rheology and mechanical properties of Blast furnace slag (BFS)- fly ash binder system activated by sodium hydroxide and sodium silicate is studied considering different control factors including  $\text{Na}_2\text{O}/\text{b}$  ratio, BFS/binder and  $\text{SiO}_2/\text{Na}_2\text{O}$  ratio.  $\text{Na}_2\text{O}/\text{b}$  ratio and  $\text{SiO}_2/\text{Na}_2\text{O}$  ratio are optimized considering the rheology of the alkali activated paste (AAP). The value of BFS/b ratio is then optimized considering both rheology and mechanical behaviour of AAB system. Alkali-activated materials exhibit poor workability in mixing because of high viscosity of the paste and fast setting. This is great disadvantage considering the placing and transport of the AABs. In this study, red gypsum and phosphoric acid as additives to enhance the rheological properties ensuring that the resulting binder have strength comparable to the conventional cement mortar.

*Keywords:* Alkali activated binders, Blast furnace slag-Fly ash, Rheology, Red gypsum, Phosphoric acid, admixtures

## TABLE OF CONTENTS

Sl No.	Title	Page No.
	ACKNOWLEDGEMENT	i
	ABSTRACT	ii
	LIST OF FIGURES	v
	LIST OF TABLES	vii
1	INTRODUCTION	1
1.1	General	1
	1.1.1 Alkali Activated Binder (AAB) System	2
	1.1.2 Preparation of AABs	2
1.2	Problem Statement	3
1.3	Scope of the Work	3
1.4	Objectives of the Work	4
2	LITERATURE REVIEW	5
2.1	General	5
	2.1.1 Alkali Activated Materials	5
	2.1.2 Hardening Process	5
	2.1.3 Blast Furnace Slag-Fly Ash Based AAB	7
	2.1.4 Molarity of Alkaline Solution	9
	2.1.5 Rheology of AAB	10
	2.1.6 Effect of Control Factors	10
	2.1.7 Effect of Admixtures	13
2.2	Research Gap	15
3	MATERIALS AND METHODS	16
3.1	Materials	16
	3.1.1 Precursors	16
	3.1.2 Activator Solution	16
	3.1.3 Admixtures	18
	3.1.4 Fine aggregate	19
3.2	Methodology	19
	3.2.1 Parameters Used for the Study	21
	3.2.2 Phase 1	22
	3.2.3 Phase 2	23

3.2.4 Phase 3	24
4 EXPERIMENTAL PROGRAM	25
4.1 Mixing Protocol	25
4.2 Testing Program	26
5 RESULTS AND DISCUSSION	30
5.1 Effect of Ms Ratio and Na <sub>2</sub> O/b Ratio	30
5.1.1 Effect on Setting Time	30
5.1.2 Effect on Penetration Resistance	31
5.1.3 Effect on Flowability and Slump Retention	35
5.1.4 Inference	40
5.2 Effect of BFS/b Ratio	40
5.2.1 Effect on Setting Time Of AAP	40
5.2.2 Effect on Penetration Resistance Of AAP	41
5.2.3 Effect on Flowability and Slump Retention Of AAP	42
5.2.4 Effect on Density of AAM	44
5.2.5 Effect on UPV of AAM	45
5.2.6 Effect on Compressive Strength Of AAM	46
5.2.6 Effect on Flexural Strength of AAM	47
5.2.7 Inference	48
5.3 Effect of Admixtures	49
5.3.1 Inference	56
6 CONCLUSION	57
REFERENCES	59
APPENDIX 1	62

## LIST OF FIGURES

Fig No.	Title	Page No.
2.1	Reaction mechanism of geopolymerization	6
2.2	Effect of GGBS inclusion on compressive strength of alkali activated concrete	8
2.3	Compressive strength of alkali activated slag/fly ash blends at 28 days	9
2.4	Effect of BFS/binder ratio and water/binder ratio on flowability of BFS/FA-AAP	11
2.5	Initial and final setting times of SSA and SFA mixtures	12
2.6	Influences of the phosphoric acid concentration on retarding the setting times.	14
3.1	Red gypsum	18
3.2	Methodology of the Thesis Work	20
4.1	Hobart mixer	25
4.2	Mini slump cone	26
4.3	Vicat apparatus with needle for the test	27
4.4	UPV test on AAM specimen	28
4.5	Multi frame testing apparatus for flexural strength test on $40 \times 40 \times 160 \text{ mm}^3$ AAM Prism specimens	29
4.6	Digital compression testing machine for compressive strength test on $40 \times 40 \times 40 \text{ mm}^3$ cube specimens	29
5.1	Effect of Ms ratio and $\text{Na}_2\text{O/b}$ ratio on setting time of BFS-FA AAP	31
5.2	Variation of penetration resistance with $\text{Na}_2\text{O/b}$ (%)	33
5.3	Variation of penetration resistance with Ms ratio	35
5.4	Effect of Ms ratio and $\text{Na}_2\text{O/b}$ ratio on flowability of GGBS-FA AAB	36
5.5	Effect of Ms ratio on flowability of GGBS-FA AAB	37
5.6	Effect of $\text{Na}_2\text{O/b}$ ratio on flowability of GGBS-FA AAB	39
5.7	Effect of BFS/b ratio on setting time of GGBS-FA AAB	41
5.8	Variation of penetration resistance with BFS/b ratio for $\text{Ms}=1.5$ and $\text{Na}_2\text{O/b}=6\%$	42

5.9	Effect of BFS/b ratio on the flowability of GGBS-FA AAB	43
5.10	Effect of BFS/b ratio on flowability of GGBS-FA AAB for Ms=1.5 and Na <sub>2</sub> O/b=6%	43
5.11	Variation of density of AAM specimens with BFS/b ratio	44
5.12	Effect of BFS/b on UPV of AAM	45
5.13	Effect of BFS/b on compressive strength of AAM	46
5.14	Effect of BFS/b on flexural strength of AAM	47
5.15	Setting time test on AAP with 0.8M phosphoric acid and red gypsum	49
5.16	Setting time test on AAP of 100% slag with 0.8M phosphoric acid and red gypsum at 2.5% of binder content	50
5.17	Setting time test on AAP with 0.8M phosphoric acid as admixture	51
5.18	Effect of red gypsum on setting time of BFS-FA AAP	52
5.19	Setting time test on AAP with 0.5M phosphoric acid and red gypsum at 2.5%	53
5.20	Variation of setting time with the molarity of phosphoric acid for BFS-FA AAP of BFS/b ratio 0.5 and red gypsum of 2.5%	54
5.21	Variation of setting time with the molarity of phosphoric acid for BFS-FA AAP of BFS/b ratio 0.75 and red gypsum of 2.5%	55

## LIST OF TABLES

Table No.	Title	Page No.
3.1	Chemical composition of sodium hydroxide	17
3.2	Chemical Composition of Sodium Silicate	18
3.3	Chemical Composition of Phosphoric acid	19
3.4	Control factors and the values considered for different phases of the study	21
3.5	Values of Ms and Na <sub>2</sub> O/b used for AAP mixes for phase 1	23
3.6	BFS and FA content for different BFS/b ratios used in AAB system for phase 2	24
3.7	Different combination mixes with red gypsum and phosphoric acid as admixtures	24
5.1	IST and FST of BFS-FA AAP with various combinations of admixtures	54
i	Mix roportion of AAP for phase 1 experiments for 100g binder and w/s ratio of 0.4	62

## NOTATIONS AND ABBREVIATIONS

A	: Loaded surface area
AAB	: Alkali activated binders
AAFA	: Alkali-activated fly ash
AAM	: Alkali activated mortar
AAP	: Alkali activated paste
AAS	: Alkaline activator solution
AAS	: Alkali-activated slag
AASC	: Alkali activated slag cement
AS	: Aluminosilicate
b	: Mass of both GGBFS and FA
BFS	: Blast furnace slag or mass of GGBFS
FA	: Fly ash
$f_m$	: Compressive strength
FST	: Final setting time
GGBFS	: Ground granulated blast furnace slag
GPM	: Geopolymer mortars
IST	: Initial setting time
$M_s$	: Activator modulus
$Na_2O$	: Sum of $Na_2O$ in the activators
OPC	: Ordinary portland cement
P	: Maximum load
s	: Total solid content from precursors, activators and admixtures
SFA	: Sodium silicate activators
$SiO_2$	: Silica equivalent in sodium silicate activator
SSA	: Silica fume activators
UPV	: Ultrasonic pulse velocity
w	: Sum of water from both activators and additional tap water
WG	: Waterglass
$\delta_f$	: Flexural strength

# CHAPTER 1

## INTRODUCTION

### 1.1 GENERAL

Due to the quick growth of infrastructure, there is a significant need for cement manufacturing worldwide. However, the increasing manufacturing of cement also results in an increase in the amount of greenhouse gas emissions that are produced during its production. A tonne of CO<sub>2</sub>, a greenhouse gas that contributes to global warming, is released during the manufacturing of one tonne of Portland cement. The manufacturing of Portland cement is responsible for more than 7% of global CO<sub>2</sub> emissions. Furthermore, CO<sub>2</sub> makes up around 65% of greenhouse gases that cause global warming. As a result, the Portland cement business does not match the idealised contemporary vision of a sustainable industry. To make the construction business environmentally sustainable, a substitute for Portland cement must be found immediately. The new binder material must, however, also have adequate strength and durability qualities that are on equal with or, preferably superior than those of conventional concretes made of Portland cement.

Alkali-activated binders have received a lot of attention as a part of environmentally friendly cementing binder systems. Numerous aluminosilicate precursors with varying levels of availability, reactivity, cost, and value can be used to produce these binders. The local accessibility of acceptable raw materials (precursors and activators) is the primary aspect that is likely to affect the likelihood of uptake and utilisation of alkali-activated binders in any particular place. Because alkali-activated materials can minimise CO<sub>2</sub> emissions as well as industry waste management, using them instead of cement-based products has significant economic and environmental advantages. While using alkali-activated materials, the competition for raw materials must also be taken into account since many of the precursors used to make alkali-activated binders are also sought after for use in blends with Portland cement. If alkali-activated materials are to be marketed as an environmentally friendly choice, bulk material transportation must obviously be reduced, as doing so can significantly increase the carbon footprint of the binder as a whole.

### **1.1.1 ALKALI ACTIVATED BINDER (AAB) SYSTEM**

Alkali activation is the process of transforming a solid aluminosilicate (AS), known as the "precursor," into a hardened binder made of hydrous alkali and aluminosilicate under alkaline conditions produced by the "alkali activator". Many different by-products and waste products from various industrial processes are employed as precursor materials. Some of the precursors require grinding, calcination, or thermal activation while others can be utilised directly. The three most prevalent precursor materials are metakaolin from the calcination of kaolin, fly ash from coal power plants, and slag from the manufacturing of iron. In addition, there are a wide variety of additional potential precursors, such as bottom ash from municipal solid waste incineration, red mud, waste from the production of ferronickel, volcanic and synthetic glass, phosphorous slag, copper and zinc slag, and rice husk ash. The activator is the second essential part of AAB. Its function is to facilitate the development of early-age strength and increase the pozzolanic reactivity of aluminosilicate powder. The activators for AABs are based on an alkaline metal, Na or K, and an anionic group, with hydroxide and silicate being the most popular, but carbonate and sulphate are also relatively common. (Serdar et al. 2021).

### **1.1.2 PREPARATION OF AABS**

Strong alkaline solutions like sodium hydroxide (NaOH) and potassium hydroxide (KOH), as well as soluble silicates (most of them), such as gelatine silicate, are used to trigger an alkaline source material rich in ASs in the presence of proper curing environments. The raw ingredients go through geopolymerization in the presence of an alkaline media to create an amorphous to semicrystalline structure, which ultimately results in higher strength or composite material that is similar to ordinary concrete. Precursor and alkaline activator coupling must be taken into account in order to obtain good product efficiency; due to the differences in composition, most precursors will either react preferentially or operate efficiently with particular types of activators.

Alkali-activated binders can be created in one of two ways: as a one-part mix (dry powder and water) or as a two-part mix (dry powder and liquid activator). The majority of the goods now on the market are made using the two-part mix type, which is likely to be the primary approach used in the initial deployment of alkali-activation in most countries. One-part systems, however, are probably going to become a more scalable technology in the future due to the potential for factory production and distribution as a bagged material, once this

technology is developed and other concerns connected to the typically poor strength development of one-part mixtures are handled. For precast construction, where chemical handling and curing schedules can be more precisely controlled, the two-part combination seems to be more likely to be scaleable (Provis 2018).

## **1.2 PROBLEM STATEMENT**

Alkali activated binders can be used as an alternative to traditional concrete. The rheology of AAB is extremely complicated and is affected by a wide range of factors, including the ratio of water to solid, the presence of precursors and activators, temperature, and curing time. Due to the early development of Calcium-silicate hydrate (CSH) gel due to the availability of  $\text{Ca}^{2+}$  ions, the majority of AAB has very poor workability and a quick setting time. Therefore, it is necessary to research how various elements impact the rheology of the binder. Admixtures that control rheology can be utilised for this. It is necessary to increase the setting time, workability, and flowability of AAB systems without sacrificing the strength.

## **1.3 SCOPE OF THE WORK**

This study only uses blast furnace slag and class F fly ash as the precursor materials and Sodium hydroxide and sodium silicate as activators. There is a wide range of precursors and activators available which when used in different combination shows different properties. This study focuses on workability and setting time as rheological properties. The Properties of the alkali activated Slag-fly ash paste and mortar is only considered for the study. It can be further extended to alkali activated Slag-fly ash concrete. The behaviour of AAB depends on parameters like  $\text{Na}_2\text{O}$ /binder ratio, the  $\text{SiO}_2/\text{Na}_2\text{O}$  ratio, the water/solid ratio, and the BFS/binder ratio. In this study the influence of BFS/binder ratio,  $\text{Na}_2\text{O}$ /binder ratio, the  $\text{SiO}_2/\text{Na}_2\text{O}$  ratio on the behaviour of blast furnace slag-flyash (BFS-FA) based AAB system is considered, keeping other water/solid ratio constant.

#### **1.4 OBJECTIVES OF THE WORK**

- To investigate the effect of  $\text{Na}_2\text{O}$ /binder ratio and activator modulus (Ms) on the rheology of BFS-FA based Alkali Activated Paste (AAP) at BFS/binder ratio of 0.50 and to identify an optimum  $\text{Na}_2\text{O}$ /binder ratio and activator modulus (Ms) based on rheology of AAP.
- To evaluate the influence of BFS/binder ratio on the rheology of BFS-FA based Alkali Activated Paste (AAP) and mechanical properties of Alkali activated mortar (AAM) at optimum  $\text{Na}_2\text{O}$ /binder ratio and activator modulus (Ms) based on rheology of AAP.
- To identify the combined effect of red gypsum and phosphoric acid on the rheology of AAP at optimum values of  $\text{Na}_2\text{O}$ /binder ratio, BFS/b and activator modulus (Ms).

## CHAPTER 2

### LITERATURE REVIEW

#### 2.1 GENERAL

This chapter contains brief review on alkali activated material, hardening process, blast furnace slag-fly ash based AABs, rheology of AABs and admixtures

##### 2.1.1 ALKALI ACTIVATED MATERIALS (AAMs)

Alkali activation is the general term used to describe the reaction of a solid aluminosilicate (referred to as the "precursor") under alkaline conditions (induced by the "alkali activator") to produce a hardened binder that is composed of a mixture of hydrous alkali-aluminosilicate and/or alkali-alkali earth-aluminosilicate phases. Alkali activation is theoretically possible with any raw materials that contain reactive aluminium and silica. Alkaline activator solutions and solid raw materials are typically combined to create alkali activated materials. Another name that is frequently used in relation to these materials is the phrase "geopolymer," which is mostly used to describe low-calcium alkali-activated aluminosilicate binders (Provis 2018).

Alkali activated binders are made from two major components (Rajamane et al. 2012):

- Precursor materials containing silica and alumina, which may be natural minerals (such kaolinite, clays, etc.) or industrial by-products (such as fly ash, silica fume, slag, rice-husk ash etc).
- Alkaline Activator Solution (AAS), which is often based on sodium or potassium-based alkali metals The most widely used AAS is a mixture of alkali hydroxide (NaOH, KOH) and alkali silicate (Sodium or potassium silicate).

##### 2.1.2 HARDENING PROCESS

Geopolymerisation is the term used to describe the chemical reaction between the aluminosilicate-rich material and the alkaline activators. Geopolymerization is an exothermic process. The hydroxyl ions in the alkali reactant begin to dissolve the alumino-silicates in the source material when the precursor comes into contact with the alkaline medium. The covalent bonds Si-O-Si and Si-O-Al break down into colloidal phase during this process. As a result, aluminate and silicate ions are released, which promotes additional polymerization.

The extent of the reaction is determined by the alkali medium concentration, ion exchange capability, fineness, and structure of the precursor materials. The dissolved components continue to interact, resulting in a coagulated structure. An intermediate product (Gel 1) with a high Al content changes into Gel 2, which has a higher Si content, as the reaction advances (Fig. 2.1). During curing, the gel phase undergoes continual rearrangement, resulting in the formation of additional cross-links and the expulsion of unbound water (Rangan, 2008). The gel develops and creates three-dimensional frameworks in this way.

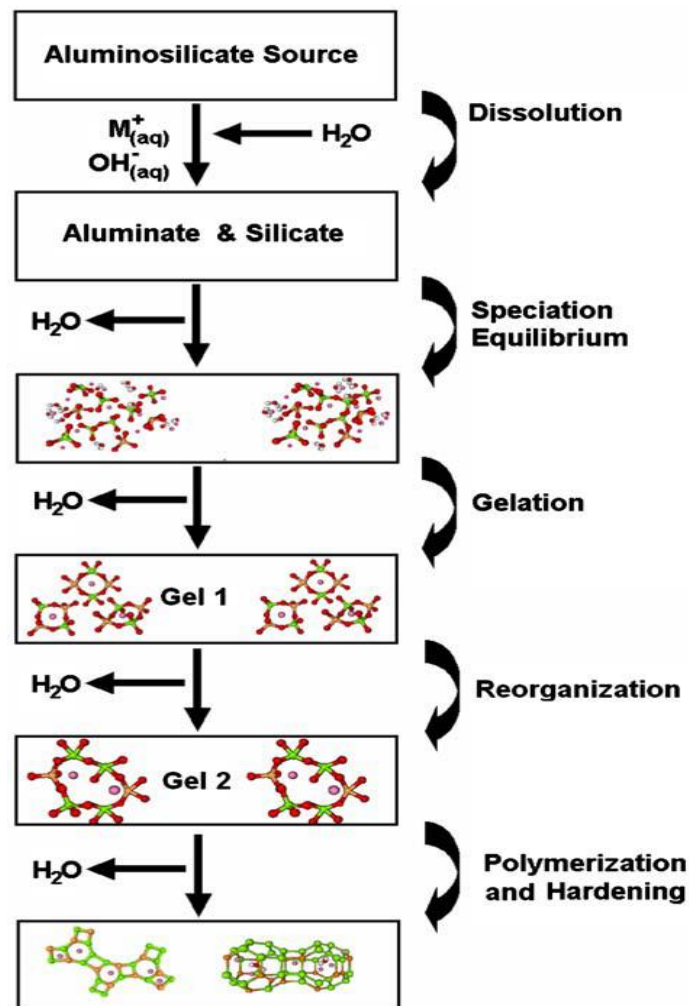


Fig. 2.1 Reaction mechanism of geopolymerization (Rangan, 2008)

The commonly acknowledged geopolymerization mechanism consists of three phases (Xu and Van Deventer, 2000):

- When an alkaline activator solution is added, aluminosilicates dissolve from the binder materials, forming Silica and alumina tetrahedral units known as precursor units.
- The precursor units are then moved, repositioned, or condensed into monomers, which are subsequently polycondensed or polymerized to create a three-dimensional structure known as a geopolymeric structure.

However, it can be challenging to determine the exact order in which the aforementioned processes occur because they can either happen one after the other or overlap, making it challenging to pinpoint and analyse what occurs separately.

Based on the final phase assemblage, AAMs may generally be divided into two categories:

- Low Ca systems - These systems are based on the activation of a low Ca precursor, such as fly ash or metakaolin, with the major reaction product being a three-dimensional alkali-aluminosilicate hydrate (N-A-S-H) type gel.
- High Ca systems - These systems are based on the activation of a high Ca precursor, such as slag, with the major reaction product being calcium-aluminosilicate hydrate (C-A-S-H) type gel.

### **2.1.3 BLAST FURNACE SLAG-FLY ASH BASED AAB**

In contrast to alkali-activated low-calcium fly ash, which must be heated and cured during preparation, alkali-activated slag and alkali-activated slag/fly ash (AAS) appear to have broader application prospects. Mehta et al. (2020) investigated the impact of partially substituting ground granulated blast furnace slag (GGBFS) for fly ash on compressive strength. Due to the additional calcium-based hydration products CSH and CASH as well as the polymerization products NASH, the inclusion of GGBFS as a partial replacement for fly ash increases the compressive strength of fly ash based alkali-activated concrete, making the matrix of alkali-activated binder more compact with fewer cracks and pore spaces. As demonstrated in Fig. 2.2, alkali-activated concrete with 20% GGBS as fly ash substitute reaches its maximum compressive strength of roughly 65 MPa at 90 days.

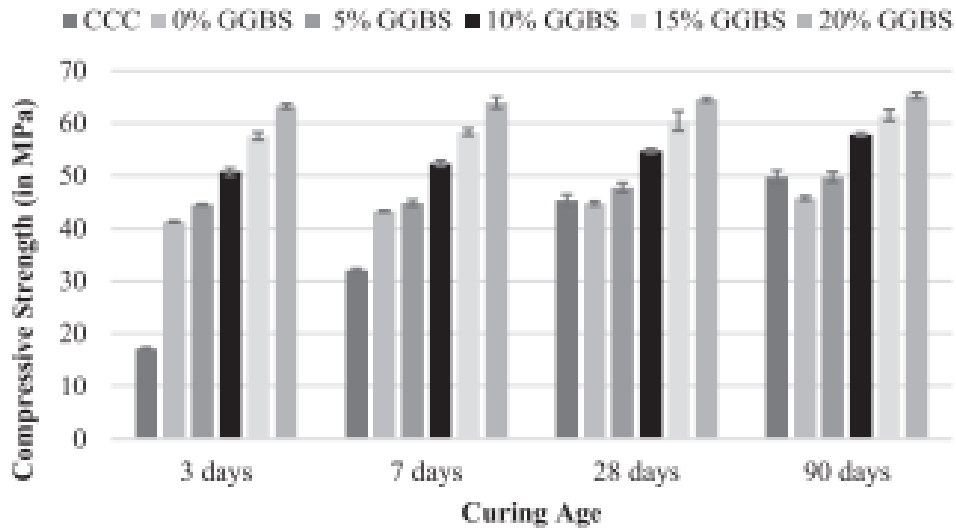


Fig. 2.2 Effect of GGBS inclusion on compressive strength of alkali activated concrete

Mehta et al. (2020)

Given how sensitive alkali activated compounds are to the composition of the beginning components, recognising their affects is critical for their use. Blends of slag and fly ash that have been alkali activated and cured at room temperature have proven advantageous in field applications. Gao et al. (2015) studied on the effects of two compositional factors: activator modulus ( $SiO_2/Na_2O$  from 1.0 to 1.8) and slag/fly ash mass ratios (between 90/10 and 50/50) on reaction kinetics, gel characters and compressive strength. The findings demonstrate that decreasing the activator modulus greatly speeds up the early age reaction and increases reaction intensity. Increasing the slag percentage also speeds up the reaction rate, especially at low activator modulus. According to the results of the compressive strength tests, the optimum activator modulus varies with the mass ratio of slag to fly ash. In general, higher slag/fly ash mass ratios prefer higher activator moduli, while too high or too low activator moduli have a negative impact on strength, as shown in Fig. 2.3. The shifts in the ideal parameters for strength suggest that the activator modulus and slag/fly ash ratio are the two most important variables to take into account in order to reach the desired strength.

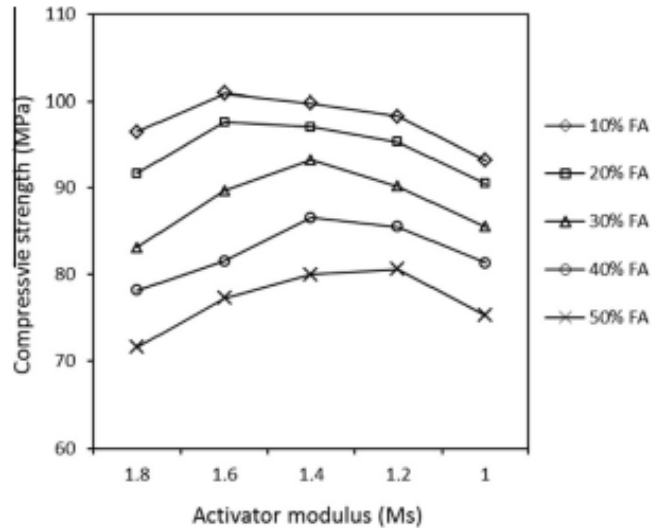


Fig. 2.3 Compressive strength of alkali activated slag/fly ash blends at 28 days

Gao et al. (2015)

#### 2.1.4 MOLARITY OF ALKALINE SOLUTION

In order to dissolve a particular proportion of silica and alumina and to facilitate the surface hydrolysis of the raw material particles, the polymerization of aluminosilicates needs a strongly alkaline media. Activators, which are simple or mixed alkaline solutions, can be used to create this type of alkaline media. It is yet unclear how altering the molarity of the activator (NaOH solution) may affect mechanical and fresh properties. Fahim et al. (2018) investigated how the molarity of the solution affected the microstructures and mechanical characteristics of multi-blend geopolymer mortars (GPMs). The influence of  $\text{Na}_2\text{O}$ ,  $\text{H}_2\text{O}$  content and solution modulus ( $\text{SiO}_2:\text{Na}_2\text{O}$ ) on the strength of GPMs was investigated. It was discovered that as the alkali content increased, the flow capacity and setting time of such GPMs decreased linearly. The GPM mixtures that are activated with a high molarity NaOH solution showed a very quick setting time. The higher the molarity of NaOH, the higher the  $\text{Na}_2\text{O}$  concentration and the rate of geopolymerization action, resulting in a shorter setting time. However, as the alkali content rises, the density, split tensile, and flexural strengths all increase. The highest compressive strength, tensile strength, and flexural strength were achieved by samples made with 12M NaOH. Increased pH in samples that have been treated with 12 M NaOH solution aids in the development of the amorphous phase. The dissolution of Si and Al ions was insufficient at lower alkali concentrations, which reduced the degree of geopolymerization and the growth of mechanical strength.

Kathirvel (2015) investigated the strength development of geopolymer concrete at different slag replacement levels with metakaolin and varied alkaline concentrations and discovered that the compressive strength of the geopolymer mixes increased with increasing NaOH concentration without metakaolin. There is no substantial variation in the compressive strength of the geopolymer mixes due to the presence of metakaolin content at high sodium hydroxide concentrations. With an increase in NaOH concentration, the mixes' split tensile strength drops. Additionally, it was found that the strength was greatest for the mixture with a 12M NaOH concentration and a 20% substitution of metakaolin.

### **2.1.5 RHEOLOGY OF AAB**

The rheology of AAB is extremely complicated and is affected by a wide range of factors, including the ratio of solid to liquid, the presence of precursors and activators, temperature, and curing time. Due to the early development of CSH gel due to the availability of  $\text{Ca}^{2+}$  ions, the majority of AAB has extremely poor workability and a quick setting time. Alonso et al. (2017) investigated the effect of the precursor, the kind and concentration of the alkaline activators, and the aggregate content on the workability and rheology of alkali-activated slag (AAS) and fly ash (AAFA) mortars. Fluidity in AAM mortars was discovered to be related to the liquid/solid ratio and dependent on aggregate content. AAS and AAFA mortars activated with waterglass solutions showed broader spreads and improved workability than OPC mortars when in a plastic state, demonstrating the fluidizing action of waterglass.

Puertas et al. (2018) evaluated the effect of mixing duration on the behaviour of fresh and hardened AAS and OPC concretes. The findings of the OPC and AAS concrete slump and rheology tests were different, especially when the slag was activated with waterglass (WG). Longer mixing had a negative impact on rheology while only marginally increasing hardened performance in OPC and NaOH-activated AAS concretes. Longer mixing durations boosted the rheology and mechanical characteristics of WG-AAS concrete, which were necessary to breakdown the microstructure.

### **2.1.6 EFFECT OF CONTROL FACTORS**

The rheology and mechanical properties of AABs are influenced by a variety of factors. The  $\text{Na}_2\text{O}$ /binder ratio, the  $\text{SiO}_2/\text{Na}_2\text{O}$  ratio, the water/solid ratio, and the BFS/binder ratio are the controlling elements on the workability (flowability and setting time) of BFS/FA-AAP. The curing condition and the curing age are additional control elements on strength (compressive

strength and flexural strength) of BFS/FA-AAP. Sun et al. (2022) conducted a series of tests to systematically and quantitatively investigate the impacts of control factors on the early age properties, i.e., workability and strength of slag and fly ash-based alkali-activated paste (BFS/FA-AAP). Based on the findings, it is possible to increase strength while reducing workability by increasing the BFS/binder and  $\text{Na}_2\text{O}/\text{binder}$  ratios, as shown in Fig. 2.4. The workability might be improved while the strength might be slightly decreased by a higher water-to-binder ratio. Strength and workability both increase with a higher  $\text{SiO}_2/\text{Na}_2\text{O}$  ratio. However, larger  $\text{SiO}_2/\text{Na}_2\text{O}$  and  $\text{Na}_2\text{O}/\text{binder}$  ratios may prevent the development of strength. It has been established that a sealed curing environment is an easy but effective technique to guarantee the constant development of BFS/FA-AAP strength.

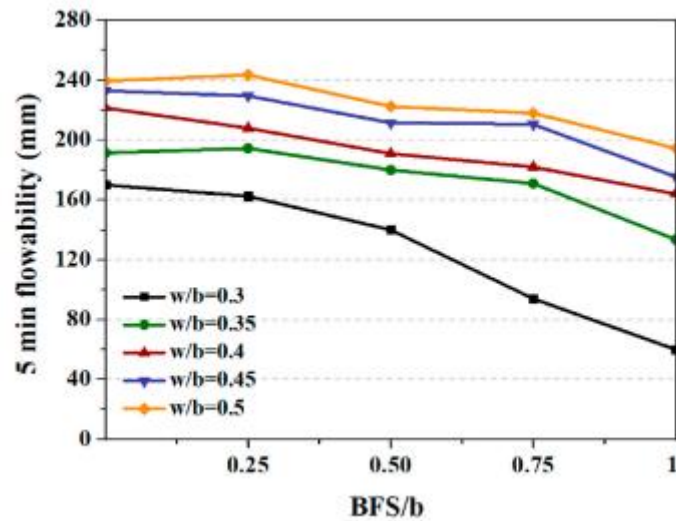


Fig. 2.4 Effect of BFS/binder ratio and water/binder ratio on flowability of BFS/FA-AAP ( $\text{Na}_2\text{O}/\text{b} = 0.5$ ;  $\text{SiO}_2/\text{Na}_2\text{O} = 1.5$ ) (Sun et al. 2022).

Dai et al. (2022) studied the effects of silica fume and sodium silicate-based activators (SFA and SSA, respectively) with varied solution modulus ( $\text{SiO}_2/\text{Na}_2\text{O}$ ) values on the setting behaviour, rheology, mechanical, and microstructural aspects of alkali activated slag cement (AASC). The findings of the setting time test demonstrated that, in contrast to SSA activation, the setting time of AASCs activated by SFA considerably increased with an increase in Ms value as shown in Fig. 2.5. In comparison to the mixtures created by SSA, the mixture produced by SFA with a Ms value of 1.2 showed fewer micro-cracks and a well-packed microstructure.

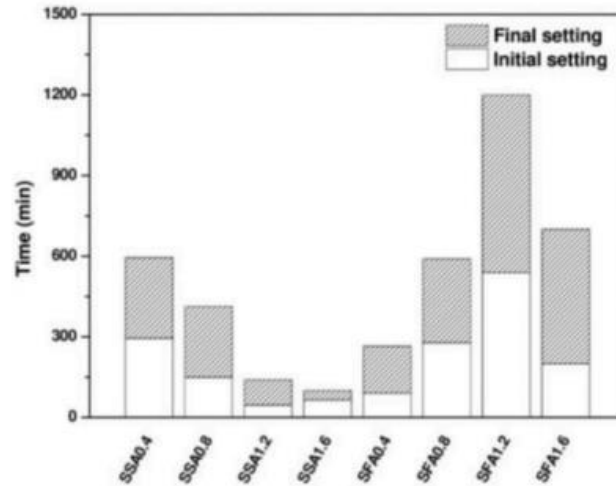


Fig. 2.5 Initial and final setting times of SSA and SFA mixtures (Dai et al. 2022).

Dai et al. (2020) investigated the impact of water to binder (w/b) ratio on the rheology and fresh state properties of alkali-activated cement (AAC) pastes. Sodium hydroxide and sodium silicate were used in three different w/b ratios of 0.32, 0.37, and 0.42 to activate a blend of 50% type F fly ash (FA) and 50% ground granulated blast furnace slag (GGBFS). The findings indicated that greater w/b ratios resulted in structural build-up at a faster rate than lower w/b ratios. Comparing AAC combinations to regular Portland cement mixtures, it was discovered that the w/b ratio had less of an impact on the setting times. It is discovered that a w/b ratio of 0.42 has the highest workability till 40 minutes.

Bocullo et al. (2021) investigated the effect of different  $SiO_2/Na_2O$  ratios on the compressive strength, chemical composition, crystallinity of hydroxy-sodalite (by-product of alkali activation), and structure of alkali activated fly ash binder. It was determined that the ratio of  $SiO_2/Na_2O$  has a significant impact on the characteristics of alkali activated material. When the ratio of  $SiO_2/Na_2O$  is less than 2, the body receives an excessive amount of sodium, which triggers the synthesis of sodium carbonate (natrite  $Na_2CO_3$ ) quickly. As a result, alkalis that are meant to produce the major byproduct of alkali activation (N-A-S-H gel) participate in the carbonation reaction and compressive strength diminishes. The ideal  $SiO_2/Na_2O$  ratio from the perspective of compressive strength is in the range of 1.5 to 2.3. (compressive strength on 28th day from 42.33 to 56.43 MPa). AAB has the highest compressive strength of 56.16 MPa on the 28th day with a  $SiO_2/Na_2O$  ratio of 2.0. Too high  $SiO_2/Na_2O$  ( $\geq 3.1$ ) does not provide sufficient alkalis for alkali activation of all amorphous alumina silicates in raw materials, resulting in a weaker structure.

Athira et al. (2021) investigated the effects of ambient, heat, water, and other curing procedures on the performance of alkali-activated binders based on slag, fly ash, and a few other precursors. Critical comparisons are made between the effects of various replacement levels for precursors, curing times, and activator concentration on the mechanical and durability qualities of alkali-activated concrete subjected to diverse curing techniques. Slag-based alkali-activated binders with ambient curing showed more strength gains than fly ash-based binders with ambient curing. High temperatures are necessary to start the reaction in fly ash-based binders, and for both slag and fly ash-based binders, higher temperatures during curing ensured greater early strength gains. Slag contributes to early-age strength, but fly ash contributes to later-age strength, making a combination of slag and fly ash preferable. Due to the leaching of the activator, water curing of alkali-activated binders is not a widely used technique.

### **2.1.7 EFFECT OF ADMIXTURES**

The early reaction process of alkali-activated slag (AAS) systems is substantially faster than that of Portland cement systems, resulting in rapid setting. As a result, fluidity control and setting adjustment are two crucial challenges for the practical uses of AAS; these problems are typically solved using chemical admixtures. Tong et al. (2021) examined current research development in the field of chemical admixtures to increase the workability and setting time of AAS systems. The characteristics of alkaline activators have a big impact on how well the polymers work. Tartaric acid and  $\text{CaSO}_4$  can both greatly slow down the hydration of NaOH-activated slag. Both boric acid/borax and phosphoric acid/phosphate are retardants appropriate for AAS systems.

Chang (2003) employed phosphoric acid as a retarder in sodium silicate-activated slag systems and discovered that the retardation was highly sensitive to the concentration of phosphoric acid, with negligible effect at a concentration of 0.78 M  $\text{H}_3\text{PO}_4$  and a minimal impact between 0.78 M and 0.84 M. As shown in Fig. 2.6, the setting time increased noticeably as the phosphoric acid concentration increased when the  $\text{H}_3\text{PO}_4$  concentration exceeded 0.84 M. Even at 0.87 M, the initial setting time might exceed 6 h. The early compressive strength and dry shrinkage were both decreased and enhanced, respectively, by the addition of 0.87 M phosphoric acid.

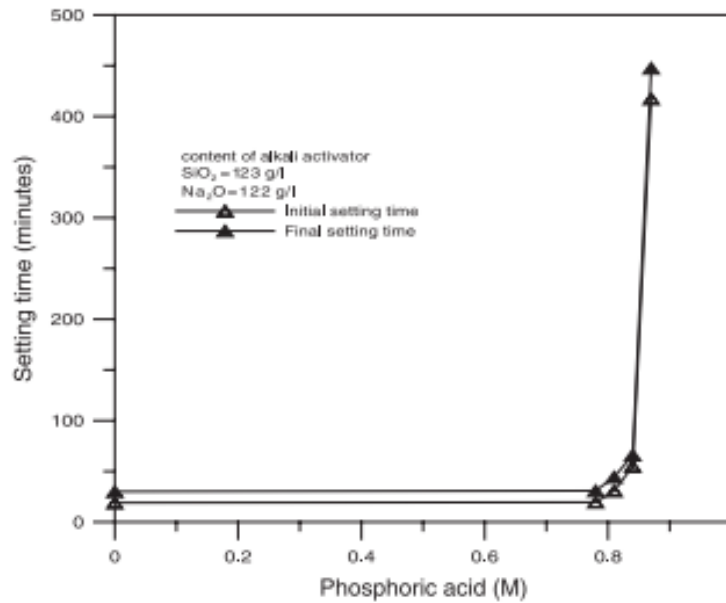


Fig. 2.6 Influences of the phosphoric acid concentration on retarding the setting times.

(Chang, 2003)

Chang et al. (2005) employed gypsum to minimise AAS shrinkage after drying. An activator based on sodium silicate was utilised. According to the results of the experiments, adding gypsum sped up the setting process, and at the same age, using more gypsum increased compressive strength. Drying shrinkage decreased when used gypsum was increased, however the findings were somewhat different when 0.82 M phosphoric acid was added to the activator along with the gypsum. The setting time was sped up by adding additional gypsum along with the phosphoric acid. Under 28 days, the compressive strength of the samples with additional gypsum was lower than that of the control samples. Drying shrinkage increased with phosphoric acid as the amount of gypsum utilised increased.

Lee and Lee (2013) studied the setting and mechanical qualities of alkali-activated fly ash/slag concrete cured at room temperature. The setting time of the alkali-activated fly ash/slag concrete was slowed down by adding phosphoric acid ( $H_3PO_4$ ) solution as a set-retarding additive. The initial setting time was seen to increase significantly and the final setting time to reduce with the addition of phosphoric acid at a weighted level of 2.0% of the total binder (fly ash + slag). However, the initial setting times increased from 15 min to 53 min and the final setting times increased from 75 min to 90 min, respectively, when the ratio of phosphoric acid to binder was increased to 2.25% by weight. Although the compressive strength of the specimen with  $H_3PO_4$  was slightly lower compared to the specimen without

$H_3PO_4$ , the inclusion of  $H_3PO_4$  was a successful method of delaying the setting of the alkali-activated fly ash/slag concrete.

Wang et al. (2020) investigated the influence of gypsum on the early hydration of slag induced by sodium hydroxide. At a constant NaOH-to-binder (slag + NaOH) ratio of 3%, NaOH was utilised as the activator (by mass of slag). Even though the initial setting was greatly delayed, gypsum greater than 3% resulted in a reduction in compressive strength. The outcomes demonstrate that  $CaSO_4$  can be used as a retarder at a certain dosage, in this case 4%. The sample had a 1-h delay in the initial setting at this level, and its compressive strength (34 MPa at 90 d) was on par with the sample devoid of  $CaSO_4$ .  $CaSO_4$  does not slow down the reaction below this point; above this point, there is significant slowing down but also a large loss in compressive strength. The retardation mechanism of  $CaSO_4$  was due to calcium ions inhibiting the dissolution of slag

## **2.2 RESEARCH GAP**

Although Slag-fly ash based alkali activated binders have been extensively studied, their properties varies significantly based on the source of the materials used. The various parameters influencing the properties of BFS/FA-AABs and their optimal values yielding good workability, setting time and strength are still under study. Studies on the effect of gypsum and phosphoric acid on the rheology and mechanical properties of slag based AABs are available. But their effect on Slag-Fly ash AAB is unknown. There is no work done on application red gypsum, an industrial byproduct with high quantity of gypsum as a rheology modifying agent.

## CHAPTER 3

### MATERIALS AND METHODS

#### 3.1 MATERIALS

Alkali activated binder mainly consists of precursor materials and activator solutions. The precursors used in the study are ground granulated blast furnace slag and class F fly ash. The activators used are sodium hydroxide and sodium silicate. Apart from these admixtures are also added which includes red gypsum and phosphoric acid. The properties of the materials used are discussed below

##### 3.1.1 PRECURSORS

AAB systems used in this research are based on ground granulated blast furnace slag (GGBFS) and fly ash as precursors. GGBFS is taken at 0, 25, 50, 75 and 100% of the total binder content (GGBFS and FA).

- GROUND GRANULATED BLAST FURNACE SLAG

Due to its strong reactivity, ground granulated blast furnace slag (GGBFS) is regarded as one of the most desirable raw materials for alkali activation. The BFS used has a specific gravity of 2.9. A dense microstructure, a high compressive strength, outstanding durability, and great environmental performance are all characteristics of alkali-activated GGBFS binders in general. However, the freshly alkali-activated GGBFS paste typically sets quickly.

- FLY ASH

Fly ash used in this study is low-calcium (ASTM Class F) fly ash. The specific gravity of fly ash used is around 2.2. The presence of calcium in fly ash in significant quantities could interfere with the polymerization setting rate and alters the microstructure. Therefore, it appears that the use of Low Calcium (ASTM Class F) fly ash is more preferable than High Calcium (ASTM Class C) fly ash as a source material to make geopolymers.

##### 3.1.2 ACTIVATOR SOLUTION

The kind of alkaline activator liquid used has also been found to be crucial to the polymerization process. The most commonly utilised alkaline liquid in geopolymerization is

a mixture of Sodium Hydroxide (NaOH) and Sodium Silicate (Na<sub>2</sub>SiO<sub>3</sub>) or Potassium Silicate (K<sub>2</sub>SiO<sub>3</sub>). In general, the alkaline liquid NaOH dissolves minerals more thoroughly than the acidic KOH, and the addition of Na<sub>2</sub>SiO<sub>3</sub> to the NaOH solution improves the reaction between the source material and the solution. As a result, the combination of Na<sub>2</sub>SiO<sub>3</sub> and NaOH is regarded as an alkaline solution in this study.

- **SODIUM HYDROXIDE**

In this study, sodium hydroxide pellets are used. Table 3.1 provides information on the chemical composition of the sodium hydroxide employed in the investigation. The molarity of the NaOH solution employed has a significant impact on the generation of reaction products. Previous research has shown that alkali activated binders with 12M NaOH solution produce the best strength characteristics. (Fahim et al. (2018); Kathirvel (2015)). Hence 12M NaOH solution is used for preparing activator solution for this study.

Table 3.1 Chemical composition of sodium hydroxide

<b>Assay</b>	97%
<b>Carbonate(Na<sub>2</sub>CO<sub>3</sub>)</b>	2%
<b>Chloride (Cl)</b>	0.01%
<b>Sulphate (SO<sub>4</sub>)</b>	0.05%
<b>Lead (Pb)</b>	0.001%
<b>Iron (Fe)</b>	0.001%
<b>Potassium (K)</b>	0.1%
<b>Silicate (SiO<sub>2</sub>)</b>	0.05%
<b>Zinc (Zn)</b>	0.02%

- **SODIUM SILICATE**

Liquid sodium silicate used for the study was obtained from Minar chemicals, Ernakulam. The composition of sodium silicate is shown in table 3.2. Molar ratio (SiO<sub>2</sub>/Na<sub>2</sub>O) of Na<sub>2</sub>SiO<sub>3</sub> used affects the rheology and mechanical properties of the AAB binder systems.

Table 3.2 Chemical Composition of Sodium Silicate

<b>Product Name</b>	54 Bhumi Sodium Silicate
<b>Density</b>	1.55
<b>SiO<sub>2</sub>/Na<sub>2</sub>O</b>	2.4
<b>Solid Content</b>	59.5%
<b>Water Content</b>	40.5%
<b>Iron content</b>	0.02% max

### 3.1.3 ADMIXTURES

The admixtures used in this study are red gypsum and phosphoric acid. From previous studies gypsum is found to have a retarding effect on the alkali activated binder, red gypsum a waste material of similar composition is thus used in this study.

- **RED GYPSUM**

Red gypsum (RG), a reddish brown semi-solid mud is a waste generated from a sulphate process of ilmenite ore which is rich in titanium and iron to acquire titanium dioxide. Red gypsum mainly contains hydrated calcium sulfate ( $\text{CaSO}_4 \cdot 2\text{H}_2\text{O}$ ) and iron hydroxide ( $\text{Fe}(\text{OH})_2$ ). The red gypsum used for the study shown in Fig. 3.1 has a 69%  $\text{CaSO}_4$  content and 30.94%  $\text{Fe}(\text{OH})_2$  content. Red gypsum is added at 2.5, 5, 7.5 and 10% of the binder content. For the current study, red gypsum is collected from Travancore Titanium Products Limited., Trivandrum.



Fig. 3.1 Red gypsum

- PHOSPHORIC ACID

Phosphoric acid has shown retarding effect on alkali activated slag based binder system. Previous studies show phosphoric acid visibly retard setting beyond 0.78 M  $H_3PO_4$  and compressive strength get reduced after 0.87M. Hence concentration of Phosphoric acid is taken below 0.8M for this study. The composition of phosphoric acid used for the study is shown in table 3.3.

Table 3.3 Chemical Composition of Phosphoric acid

<b>Assay</b>	88%
<b>Weight per ml at 20°C</b>	1.75g
<b>Calcium &amp; Magnesium</b>	0.01%
<b>Chloride (Cl)</b>	0.001%
<b>Sulphate (SO<sub>4</sub>)</b>	0.01%
<b>Nitrate (NO<sub>3</sub>)</b>	0.002%

### 3.1.4 FINE AGGREGATE

The fine aggregate used for the study is M-sand. The sand used is graded as per IS 650 (1991). The standard sand passing through 2mm IS sieve and retained on 90-micron IS Sieve with the following particle size distribution is used.

- Particle Size Smaller than 2 mm and greater than 1 mm- 33.33%
- Particle Size Smaller than 1 mm and greater than 500 micron- 33.33%
- Particle Size Smaller than 500 mm and greater than 90 micro- 33.33%

## 3.2 METHODOLOGY

This study aims at experimental investigation on rheology and strength of blast furnace slag-fly ash based alkali activated binder systems with admixtures. The sequence in which the study is carried out is shown in the flow chart below (Fig. 3.2). The study is divided into 3 phases:

Phase 1: Test on the rheology of alkali activated paste (AAP) to optimize  $SiO_2/Na_2O$  (Ms) ratio and  $Na_2O/b$  ratio at a BFS/b ratio of 0.5

Phase 2: Test on rheology and strength of AAB systems to optimize BFS/b ratio at the optimum values of  $\text{SiO}_2/\text{Na}_2\text{O}$  ratio and  $\text{Na}_2\text{O}/b$  ratio from phase 1

Phase 3: Test on rheology of AAP to find the effect of admixtures at the optimum values of  $\text{SiO}_2/\text{Na}_2\text{O}$  ratio,  $\text{Na}_2\text{O}/b$  ratio and BFS/b ratio

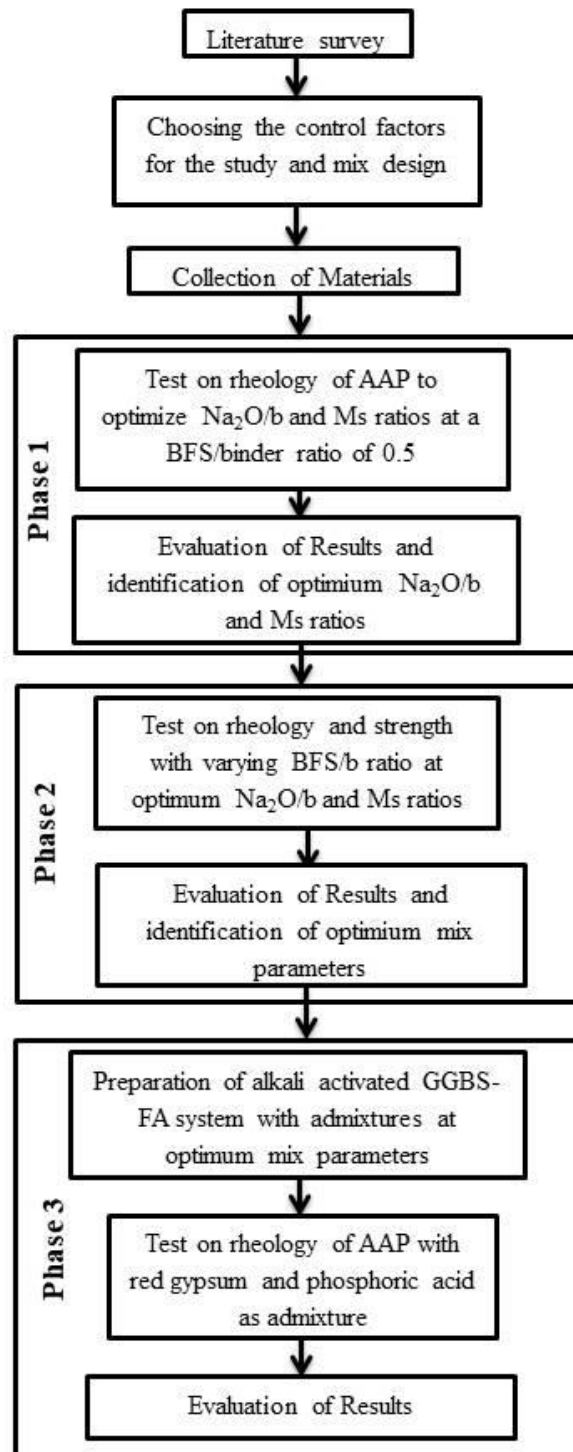


Fig. 3.2 Methodology of the Thesis Work

### 3.2.1 PARAMETERS USED FOR THE STUDY

The behaviour of AAB system is complex especially its rheology. It depends on many parameters like  $\text{SiO}_2/\text{Na}_2\text{O}$  ratio,  $\text{Na}_2\text{O}/b$  ratio,  $\text{BFS}/b$  ratio and  $w/s$  ratio. The phase 1 and 2 of the study is designed to investigate how these control factors influence both rheology and strength of the AAB system. The values of control factors used at different phases of the project are listed in table 3.4. All these ratios are mass ratios. “BFS” refers to the mass of GGBFS. “b” refers to sum of mass of both GGBFS and FA. “ $\text{Na}_2\text{O}$ ” refers to the sum of  $\text{Na}_2\text{O}$  in the activators i.e. sodium silicate and sodium hydroxide. “ $\text{SiO}_2$ ” refers to the silica equivalent in sodium silicate activator. “w” refers to sum of water from both activators and additional tap water. “s” refers to the total solid content from precursors, activators and admixtures, if any.

Table 3.4 Control factors and the values considered for different phases of the study

<b>Factors</b>	<b>Phase 1</b>	<b>Phase 2</b>	<b>Phase 3</b>
<b><math>\text{SiO}_2/\text{Na}_2\text{O}</math></b>	0,0.5,1,1.5,2	1.5	1.5
<b><math>\text{Na}_2\text{O}/b</math></b>	4%, 6%, 8%	6%	6%
<b><math>\text{BFS}/b</math></b>	0.5	0,0.25,0.5,0.75,1	0.5,0.75
<b>w/s</b>	0.4	0.4	0.4

#### BFS/b

It is the mass ratio of BFS to total binder content (BFS and FA). When the BFS/binder ratio is 0, It takes around 15 h and 4 d for the paste to reach the initial setting time and final setting time, respectively. However, it is observed that the final setting time of BFS/FA- Alkali Activated Paste (AAP) can be reached within 3 h when the BFS/binder ratio is 0.5, and an even shorter final setting time when BFS/binder is 1.0. The big difference in setting time proves that the BFS/b ratio is the dominant control factor of setting time among the control factors.

### Water/Binder

It is the mass ratio of the sum of water from both activators and additional tap water to total binder content. It is taken as 0.4 because BFS/FA-AAP is in a plastic state in all the ranges of the BFS/binder ratio. The plastic state refers to the state in which the paste will neither lose its flowability due to too little water nor has a bleeding problem due to too much water.

### $SiO_2/Na_2O$ (Ms)

Solution Modulus (Ms) is the mass ratio  $SiO_2$  (silica equivalent) in sodium silicate activator sum of  $Na_2O$  in the activator from both sodium hydroxide and sodium silicate. Previous studies concluded  $SiO_2/Na_2O$  ratio has noteworthy influence on properties of alkali activated material. The Ms Value of 0, 0.5, 1, 1.5 and 2 is used for this study

### $Na_2O/b$

It is the ratio of total  $Na_2O$  in the activators i.e. sodium silicate and sodium hydroxide to the total binder content. It depends on the molarity of the activator. The  $Na_2O/b$  ratio of 4%, 6% and 8% are used for this study

### **3.2.2 PHASE 1**

In the first phase of the thesis work, the effect of Ms ratio and  $Na_2O/b$  ratio on the rheology of BFS-FA AAP is studied. The rheology of the AAP is investigated by conducting test on setting time, penetration resistance test, flowability test and slump retention test. The value of the Ms ratio is taken as 0, 0.5, 1, 1.5 and 2 and  $Na_2O/b$  ratio is taken as 4%, 6% and 8% for this first phase of the study. The BFS/b ratio of 0.5 and w/s ratio of 0.4, as the most commonly used parameters for the research of BFS-FA AAB system, were used in phase 1 (Sun et al. 2022). The mix details are shown in table 3.5. The mix proportions of AAP mixes of phase 1 is shown in appendix 1. The main objective of phase 1 of the study is to optimize the values of Ms and  $Na_2O/b$  considering the rheology of AAP. The optimum values obtained are then used for the next phase of the work.

Table 3.5 Values of  $M_s$  and  $Na_2O/b$  used for AAP mixes for phase 1

Mix	$M_s$	$Na_2O/b$ (%)
1	0.00	4
2	0.00	6
3	0.00	8
4	0.50	4
5	0.50	6
6	0.50	8
7	1.00	4
8	1.00	6
9	1.00	8
10	1.50	4
11	1.50	6
12	1.50	8
13	2.00	4
14	2.00	6
15	2.00	8

### 3.2.3 PHASE 2

In the second phase of the thesis work, the effect of BFS/b ratio on the rheology of AAP and mechanical properties of AAM is studied. The rheology of the AAB system is investigated by conducting test on setting time, penetration resistance test, flowability test and slump retention test on AAP. The mechanical properties of the AAM is evaluated by flexural strength test, compressive strength test and ultrasonic pulse velocity (UPV) test. The BFS/b ratio is taken as 0, 0.25,0.5,0.75 and 1 for this phase 2 of the study. The optimum values of  $M_s$  and  $Na_2O/b$  that are obtained after evaluating the phase 1 results are used in this stage. The w/s ratio of 0.4 is used in this phase also. The mix details are shown in table 3.6. The

main objective of the phase 2 of the study is to optimize the BFS/b ratio of binder used so that AAB system has the most favorable behavior in the fresh and hardened state. At the end of this phase, optimum values of all the control factors, i.e. Ms Na<sub>2</sub>O/b and BFS/b ratios, are obtained. This optimum mix parameters are then used for the next phase of the study.

Table 3.6 BFS and FA content for different BFS/b ratios used in AAB system for phase 2

Sl no	BFS	FA	BFS/b
1	0%	100%	0
2	25%	75%	0.25
3	50%	50%	0.50
4	75%	25%	0.75
5	100%	0%	1

### 3.2.4 PHASE 3

In the third phase of the thesis work, the effects of admixtures on the rheology of the mix of BFS-FA AAP prepared with the optimum mix parameters are studied. The setting time of AAP is considered as the main factor to study its rheology. The admixtures used here are red gypsum and phosphoric acid. Red gypsum is added at different percentage of binder content. The molarity of phosphoric acid is also varied. The different combinations of red gypsum and phosphoric acid used are shown in Table 3.7. BFS/b ratio is also varied in the trial mixes to check its effect on setting time in the presence of admixtures. The main objective of this phase is to find the quantity of red gypsum and the molarity of the phosphoric acid required to retard the setting time of the AAP. The usage of red gypsum and phosphoric acid in conjunction is the primary focus.

Table 3.7 Different combination mixes with red gypsum and phosphoric acid as admixtures

	Mix 1	Mix 2	Mix 3	Mix 4	Mix 5	Mix 6
<b>Red Gypsum (% Binder content)</b>	2.5%, 5%, 7.5%, 10%	2.5%	0	1%, 2.5%	2.5%	2.5%
<b>Phosphoric acid (M)</b>	0.8M	0.8M	0.5M, 0.8M	0	0.25M, 0.5M	0.35M, 0.45M
<b>BFS/b</b>	0.5	1	0.5	0.5	0.5	0.5,0.75

## CHAPTER 4

### EXPERIMENTAL PROGRAM

#### 4.1 MIXING PROTOCOL

The BFS-FA AAP and AAM were prepared according to Table 3.4 according to following procedure: (1) Sodium hydroxide pellets were taken and dissolved in water to make it 12M molar concentration. (2) A day prior to casting, 12M sodium hydroxide solution and sodium silicate were combined according to the mix proportion to create the final activator solution. When the solutions are combined, a significant quantity of heat is released. (3) The solid materials i.e. precursors (BFS and FA), red gypsum (if admixtures are used) and fine aggregate (in case of AAM) were premixed for 2 min in the Hobart mixer shown in Fig. 4.1. (4) The alkali-activated solution along with additional tap water as per the mix proportions were then added and mixed for 1min. (5) In the case where phosphoric acid is used as admixture, the solution of required molarity is prepared with the additional tap water and added along with the activator solution. (6) During the 30s of rest, the layer of material adhering to the mixing arm, the walls, and the bottom of the mixing bowl was scraped and gathered. (7) The mixing process is continued for another 1 min 30s.



Fig. 4.1 Hobart mixer

## 4.2 TESTING PROGRAM

The Alkali activated GGBS-FA binder systems are tested for its rheology and mechanical properties. Test for rheology includes mini slump test, Vicat apparatus Test on Paste. Mechanical properties are evaluated using flexural strength test, compressive strength test and ultrasonic pulse velocity (UPV) test on mortar specimens

In this study, flowability and setting time is considered as the measure of rheological behavior of AAB system. The flowability of BFS-FA AAP was measured using mini slump cone (Fig. 4.2) at each time from the addition of activator till 5 min, 10 min, 15 min, 20 min, 30 min. The mini-slump test is a scaled-down version of the slump test (a top inner diameter of 38 mm, a bottom inner diameter of 62 mm, and a height of 40 mm). A slump cone was positioned in the middle of a flow table, and the fresh mixture was poured into it. The cone was raised, and the diameter of the subsided mixture was measured perpendicularly in two directions. The average value is then noted as flowability.



Fig. 4.2 Mini slump cone

Test for initial and final setting time and penetration resistance test of BFS-FA AAP was determined by using Vicat apparatus shown in Fig. 4.3. The Vicat mould was filled with the fresh mixture. Periodic penetration tests are carried out by letting a 1-mm Vicat needle to settle into this paste. The initial setting time (IST) was recorded as the time elapsed between the initial contact of raw materials and activator and the time when penetration measures to 5 mm from the bottom. For the penetration resistance test the penetration depth was recorded for every 5 mins interval till time at which the test needle fails to penetrate. For the Final setting time test needle with annular collar was used. The final setting time (FST) was recorded as the time elapsed between initial contact of raw materials and activator and the time when the needle makes an impression on the paste while the annular collar fails to do so on the paste surface.

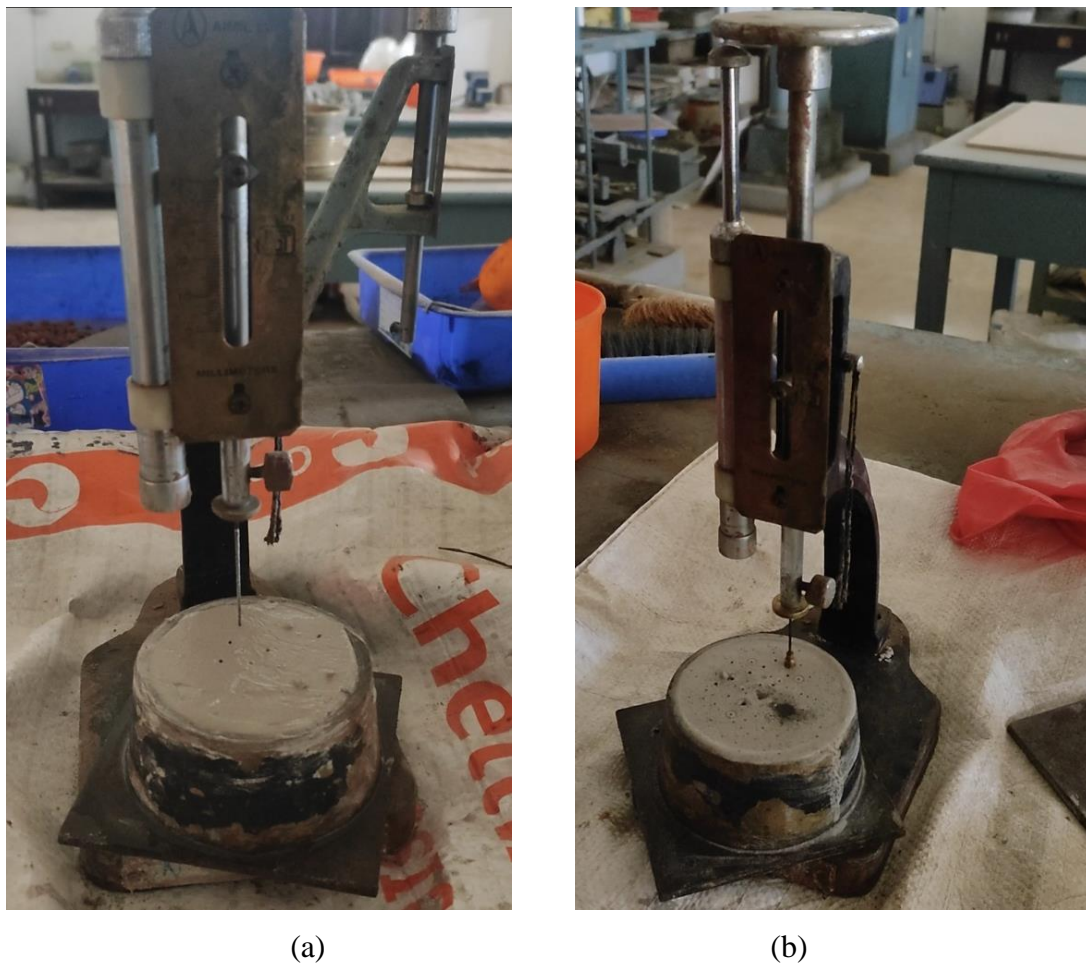


Fig. 4.3 Vicat apparatus with needle for the test for (a) IST and (b) FST

For studying the mechanical properties AAM specimens were casted after proper mixing, on moulds of dimension  $40 \times 40 \times 160 \text{ mm}^3$ . An aggregate to binder ratio of 2 was used for all mortar mixtures. All the specimens were stored in room temperature tested after 7 days and 28 days. The specimens were demoulded after 1 day, and then cured at the ambient curing conditions till the testing day. The hardened samples were subjected to UPV test, flexural strength test and compressive strength test at 7 and 28 days. The UPV test (Fig. 4.4) involves measuring the time of travel of the ultrasonic pulse through the mortar specimen and the velocity was computed by dividing the distance travelled (160mm) by the measured time. Ultrasonic pulse velocity was recorded as the average of 3 specimens.

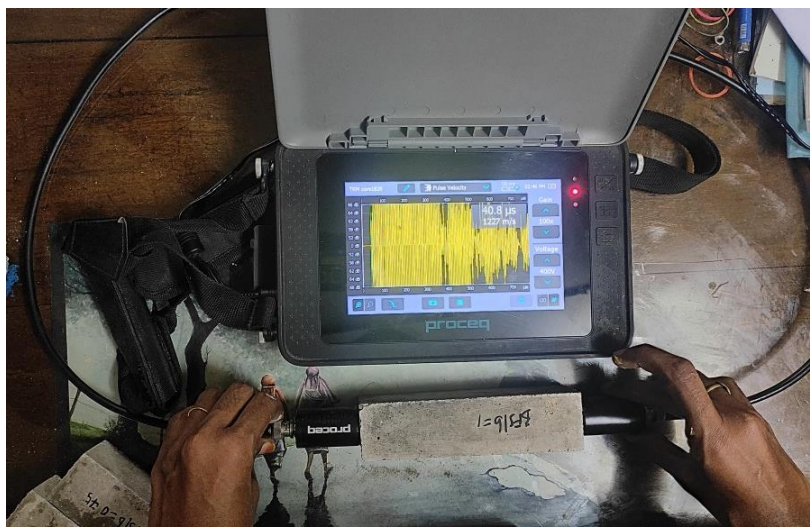


Fig. 4.4 UPV test on AAM specimen

The flexural strength is measured by a three-point bending test on multi frame testing apparatus (Fig. 4.5) according to ASTM C348 . Flexural strength was recorded as the average of 3 specimens. Flexural strength is calculated as

$$\delta_f = 0.0028P$$

Where P= Maximum load in N

$\delta_f$  = Flexural strength in MPa

After flexural strength test the two halves were used to create  $40 \times 40 \times 40 \text{ mm}^3$  cube specimens for the compressive strength test as per ASTM C349. The cubes were tested in digital compression testing machine as shown in Fig. 4.6. Compressive strength was recorded as the average of 3 specimens. Compressive Strength is calculated as

$$f_m = \frac{P}{A}$$

where  $P$ = Maximum load in N

$A$ = Loaded surface area in  $\text{mm}^2$

$f_m$ = Compressive Strength in MPa



Fig. 4.5 Multi frame testing apparatus for flexural strength test on  $40 \times 40 \times 160 \text{ mm}^3$  AAM Prism specimens



Fig. 4.6 Digital compression testing machine for compressive strength test on  $40 \times 40 \times 40 \text{ mm}^3$  cube specimens

## CHAPTER 5

### RESULTS AND DISCUSSION

#### 5.1 EFFECT OF Ms RATIO AND Na<sub>2</sub>O/b RATIO

The effect of Ms ratio and Na<sub>2</sub>O/b ratio on the rheology of AAP was observed in the phase 1 of the study. Their effect on setting time, penetration resistance, flowability and slump retention were evaluated. The optimum values of Ms ratio and Na<sub>2</sub>O/b ratio considering the rheology of AAP are obtained at the end of phase 1 which is used in the further stages of the study.

##### 5.1.1 EFFECT ON SETTING TIME

The influence of Ms ratio and Na<sub>2</sub>O/b ratio on setting time of BFS-FA AAP of BFS/b ratio 0.5 and w/s ratio 0.4 is shown in Fig. 5.1. The AAP didn't set even after 10 hrs for Ms ratio 0. With increase in Ms ratio from 0 to 1.5 the mixes showed a decrease in both initial and final setting time. More soluble Si in the system attracts more released ions, speeding reaction product production. However when Ms ratio is increased from 1.5 to 2 the setting time is increased. It is because of completely saturated Si ions in the AAP. As a result, the leftover Si ions in the precursor serve as a barrier to prevent additional reaction ions from dissolving, delaying the setting time (Sun et al. 2022).

For Ms ratio 0.5, Na<sub>2</sub>O/b ratio 4% the paste didn't set even after 10 hours. For Ms ratio 0.5, Na<sub>2</sub>O/b ratio 6% the paste took around 4 hours for initial set but the final setting didn't happen even after 10 hours. In general, with increase in Na<sub>2</sub>O/b ratio the setting time decreased indicating BFS-FA AAP with higher Na<sub>2</sub>O content tends to set faster, due to faster reaction rate.

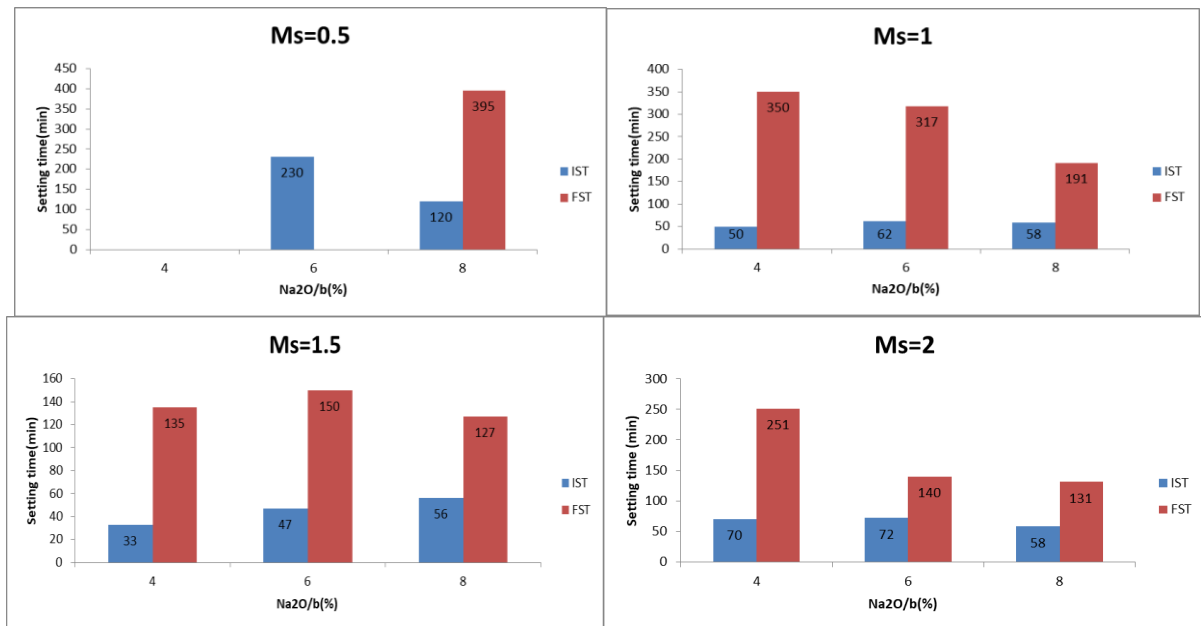
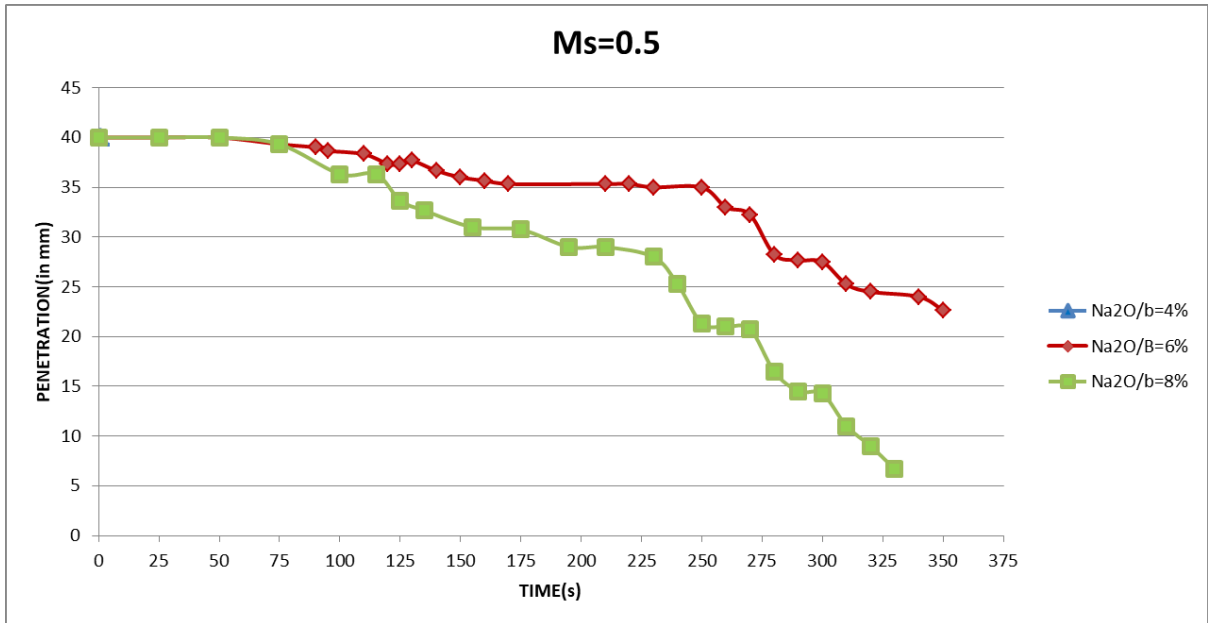


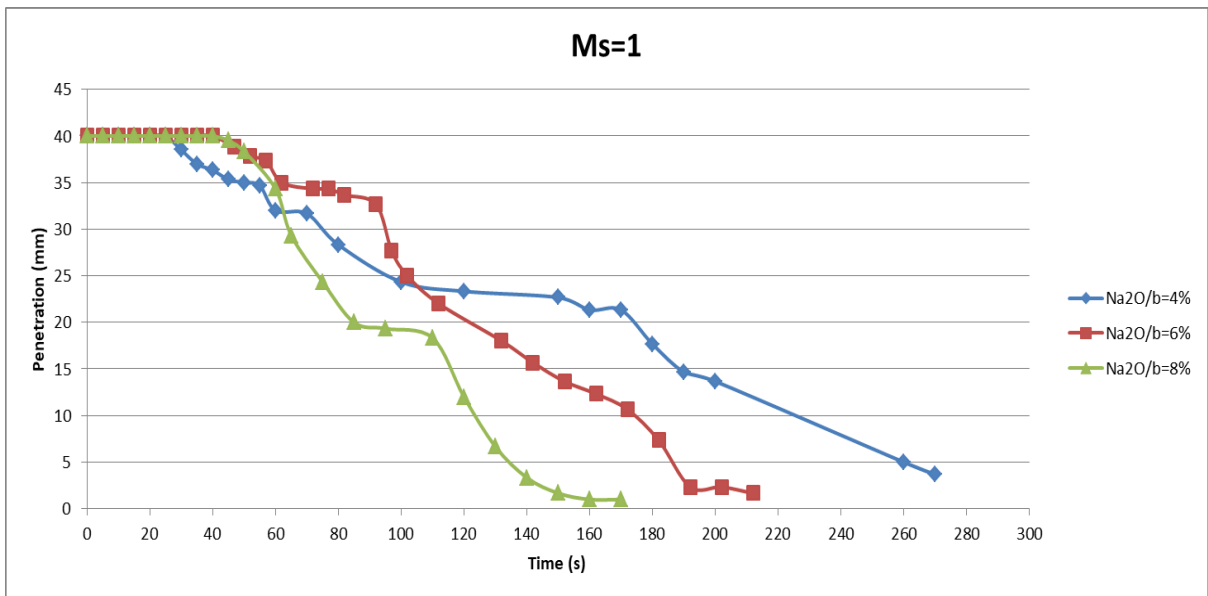
Fig. 5.1 Effect of Ms ratio and Na<sub>2</sub>O/b ratio on setting time of BFS-FA AAP

### 5.1.2 EFFECT ON PENETRATION RESISTANCE

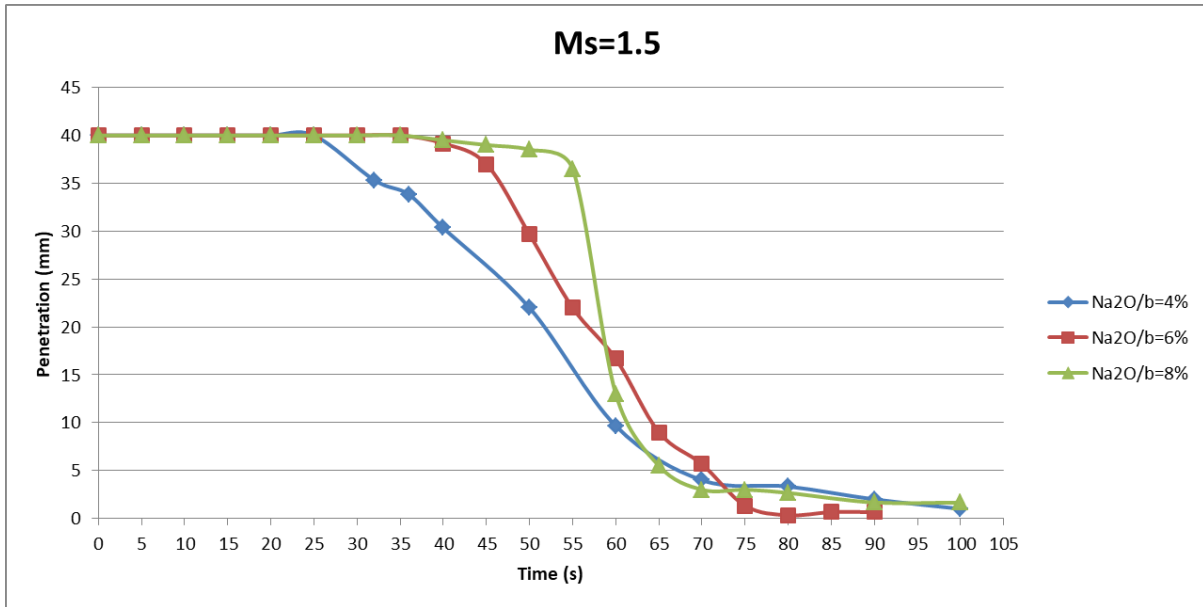
The effect of Na<sub>2</sub>O/b on the development of penetration resistance of BFS-FA AAP of BFS/b ratio 0.5 and w/s ratio 0.4 is shown in Fig. 5.2. For a constant Ms ratio the increase in penetration resistance becomes rapid with the increase of Na<sub>2</sub>O/b. The AAP sets abruptly in case of higher Na<sub>2</sub>O/b ratio. When Na<sub>2</sub>O/b is 4% the paste sets extremely slow indicating that low alkali content leads to lower concentration of OH<sup>-</sup> ion thus retarding the formation of polymerization product. On the other hand, when the Na<sub>2</sub>O/b is 8%, the penetration resistance curve obtained becomes sharp after reaching the IST, indicating a abrupt increase of penetration resistance. In case when Na<sub>2</sub>O/b is 6%, even after the IST is reached the development of penetration resistance is relatively gradual.



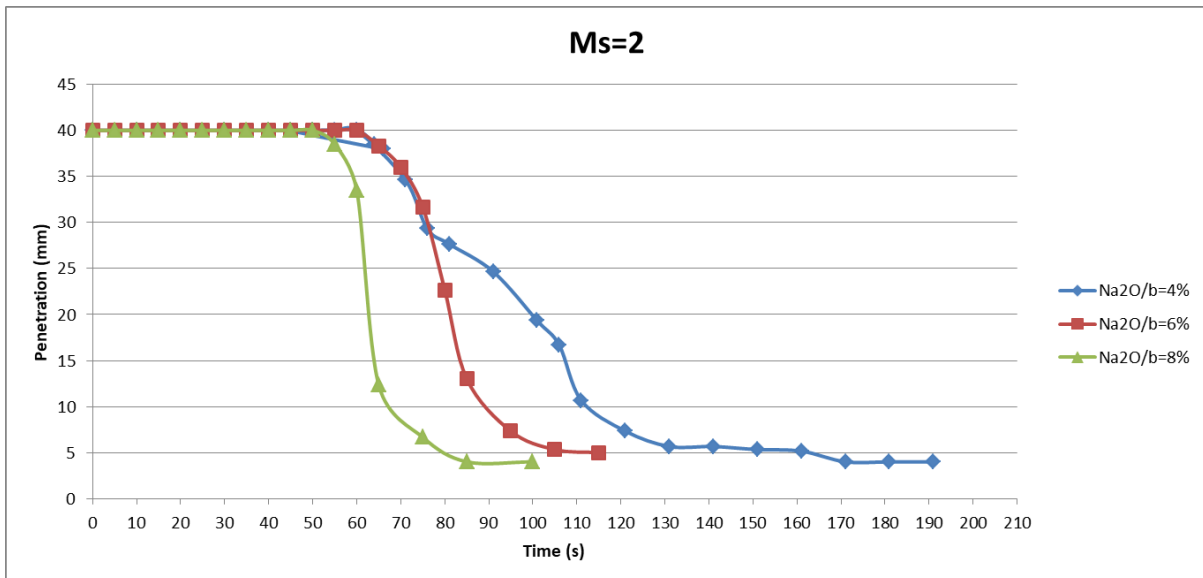
(a)



(b)



(c)

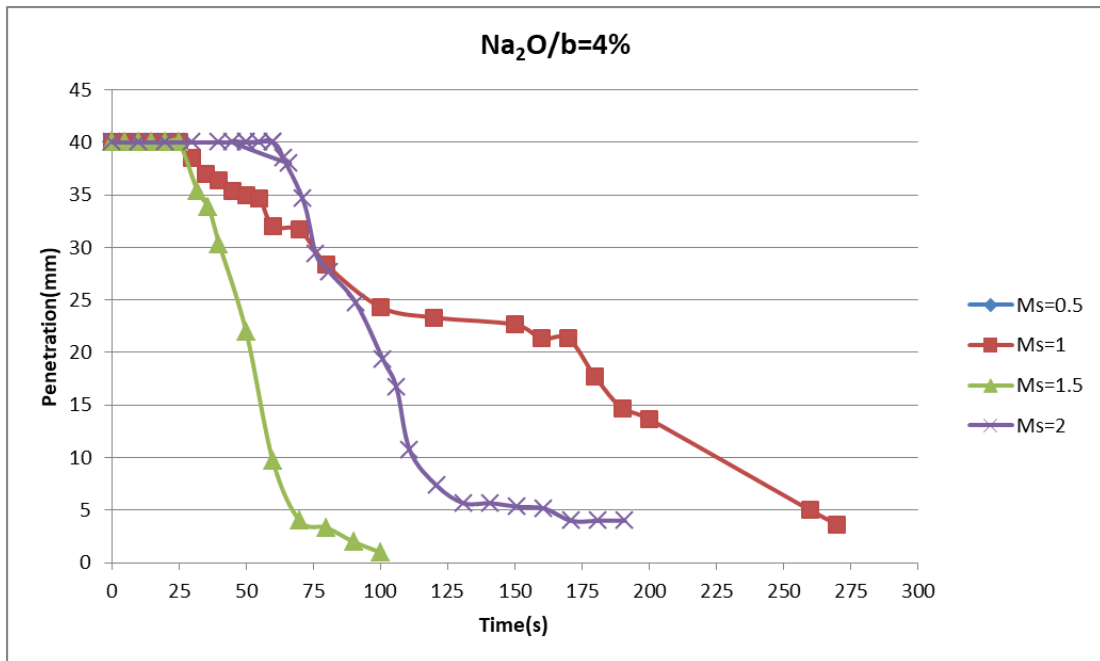


(d)

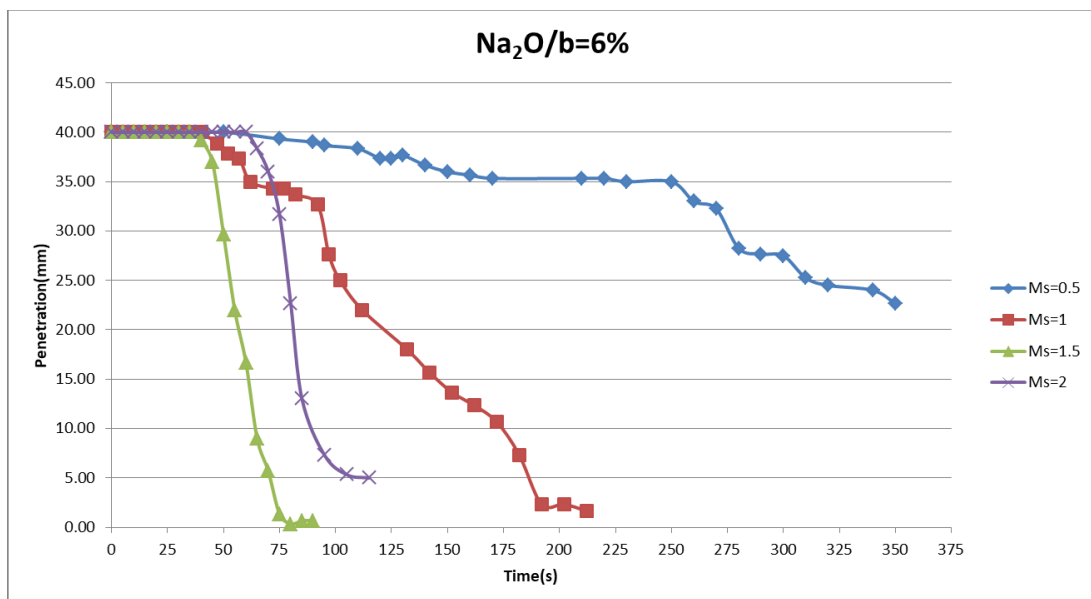
Fig. 5.2 : Variation of penetration resistance with Na<sub>2</sub>O/b (%) for (a)Ms=0.5, (b)Ms=1, (c)Ms=1.5, (a)Ms=2

Fig. 5.3 shows the influence of Ms ratio on the development of penetration resistance at a constant Na<sub>2</sub>O/b ratio of BFS-FA AAP of BFS/b ratio 0.5 and w/s ratio 0.4. For Ms ratio 0 the AAP didn't set and showed no penetration resistance even after 10 hrs. This may be attributed to lack of SiO<sub>2</sub> in the AAP, thus affecting the speed of reaction. When SiO<sub>2</sub> is introduced, with the increase in Ms ratio the paste developed penetration resistance. But when both Ms ratio and Na<sub>2</sub>O/b is low that is 0.5 and 4% respectively the paste showed no resistance to penetration. As shown in Fig. 5.3 with increase in Ms ratio till 1.5 the

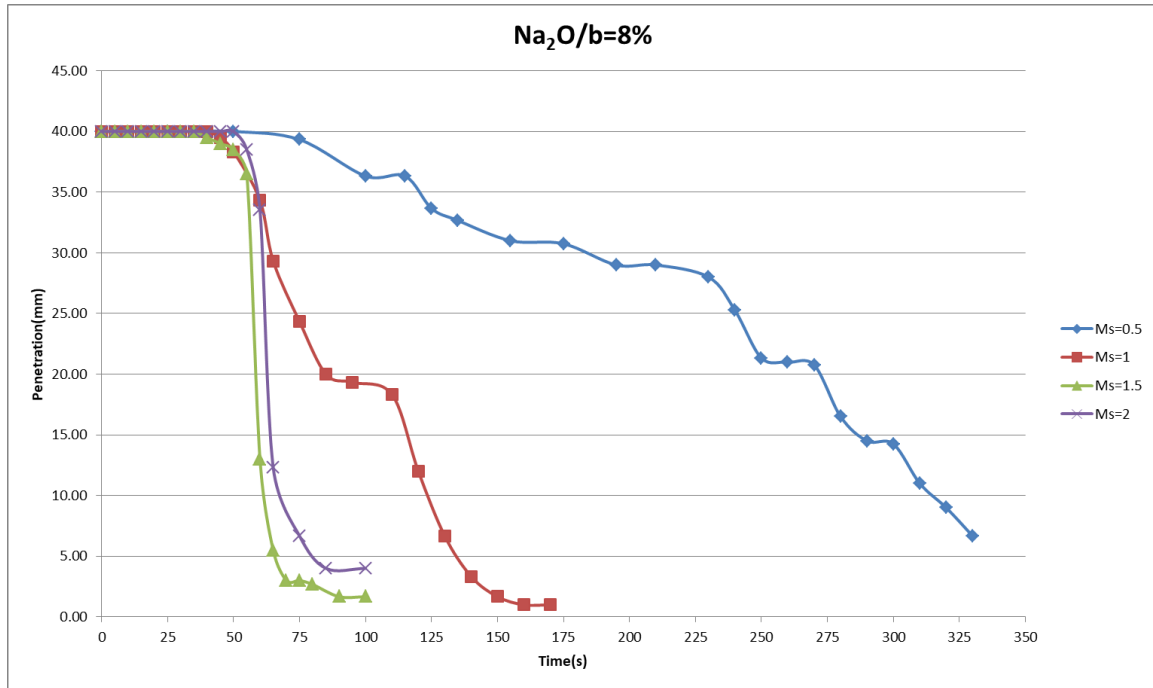
development of penetration resistance became rapid. This is because for soluble Si is introduced into the AAP which accelerates the speed of reaction. However as Ms ratio increases from 1.5 to 2 the duration of reaching maximum penetration increased. This may be due to the Si ions getting completely saturated in the AAP which in turn causes the remaining Si ions in the precursor to act as barrier for further dissolution of other reaction ions. Thus the mix with Ms ratio 1.5 exhibit a favourable time frame during which the paste remains workable.



(a)



(b)



(c)

Fig. 5.3: Variation of penetration resistance with Ms ratio with (a) Na<sub>2</sub>O/b =4%, (b) Na<sub>2</sub>O/b =6%, (c) Na<sub>2</sub>O/b =8%

### 5.1.3 EFFECT ON FLOWABILITY AND SLUMP RETENTION

Fig. 5.4 shows the influence of Ms ratio and Na<sub>2</sub>O/b ratio on the flowability of BFS-FA AAP of BFS/b ratio 0.5 and w/s ratio 0.4. The flowability increased significantly with the increase of sodium silicate in the mix. With increase in SiO<sub>2</sub> content the flowability increased. This could be as a result of the activator solution having a greater Ms ratio possibly giving the precursor particles a better coating. With an increase in the SiO<sub>2</sub>/ Na<sub>2</sub>O ratio, the flowability increases because the friction between the particles decreases (Sun et al. 2022). Due to better particle dispersion, the flowability of AAP also improves as the Na<sub>2</sub>O/b ratio rises. For instance, when Ms ratio is 1 the flow increased by 22mm and 5mm, when Na<sub>2</sub>O/b ratio is increased from 4% to 6% and 6% to 8% respectively. However when Ms ratio is increased from 1.5 to 2, the flowability increased when Na<sub>2</sub>O/b ratio is increased from 4 to 6% and decreased when Na<sub>2</sub>O/b ratio is increased from 6 to 8%. The decrease in the flowability with increase in Na<sub>2</sub>O/b can be attributed to rapid condensation. This is because the dissolution process is accelerated by the larger concentration of OH<sup>-</sup> ions, making more ions accessible for polymerization. This behaviour becomes more apparent as the concentration of SiO<sub>2</sub> increases.

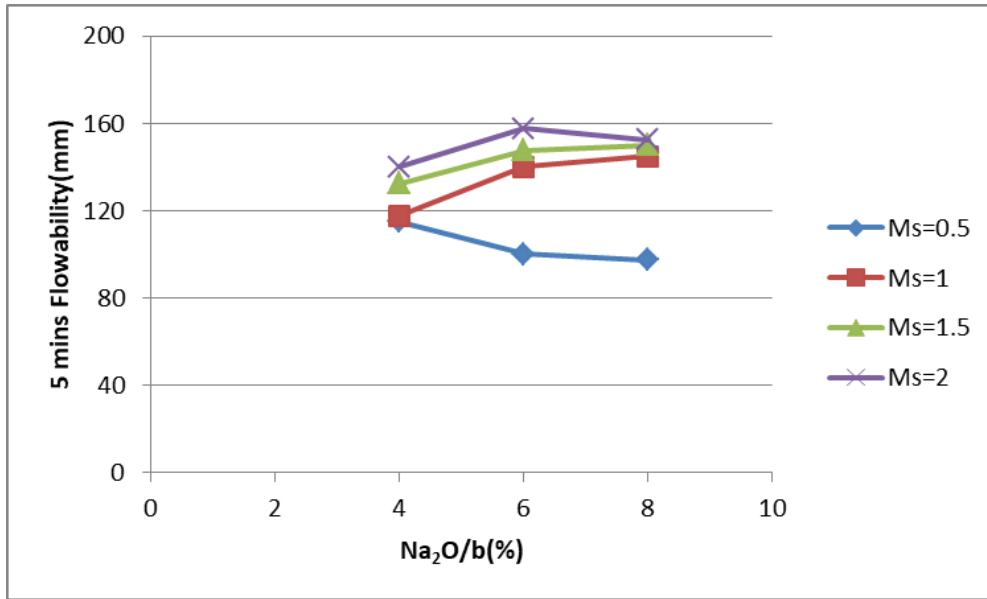
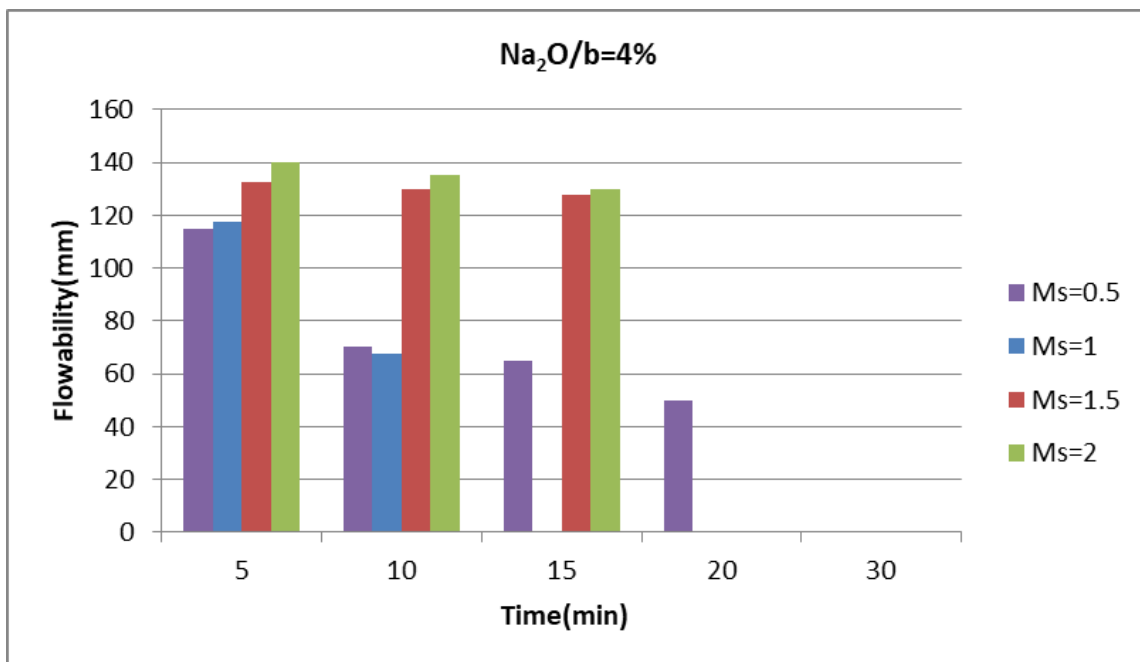
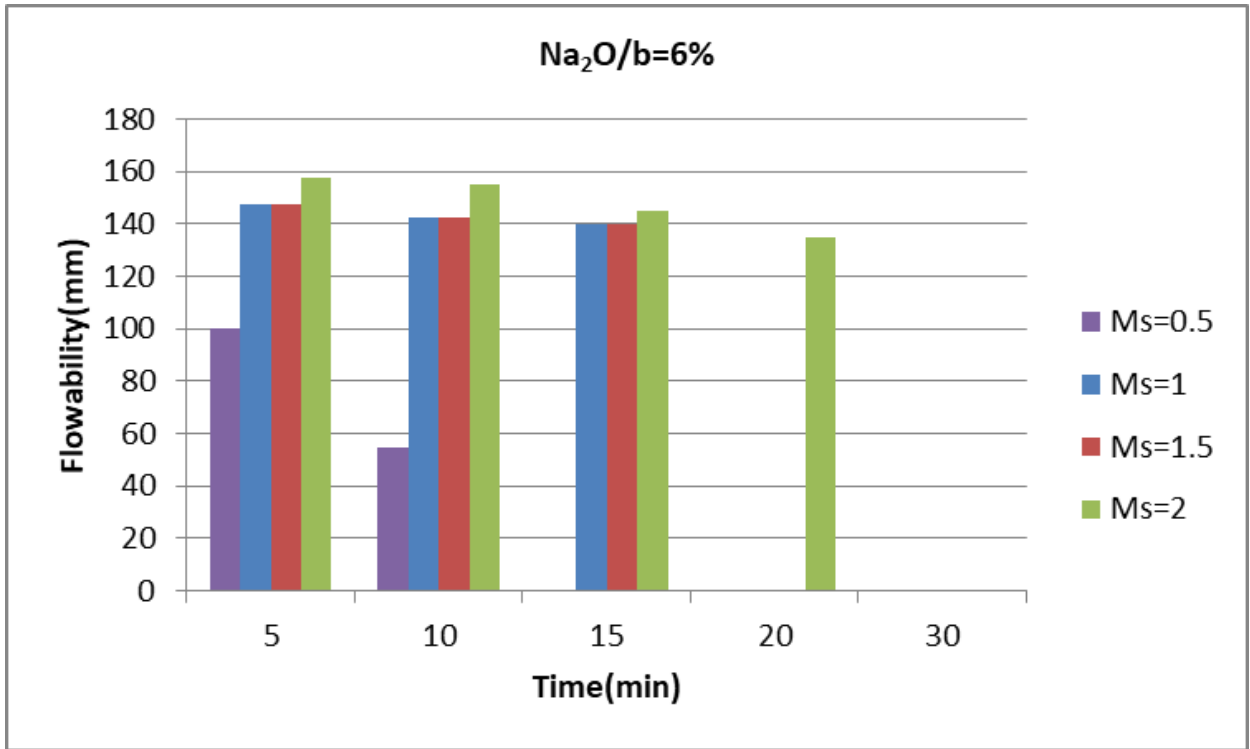


Fig. 5.4: Effect of Ms ratio and Na<sub>2</sub>O/b ratio on flowability of GGBS-FA AAB

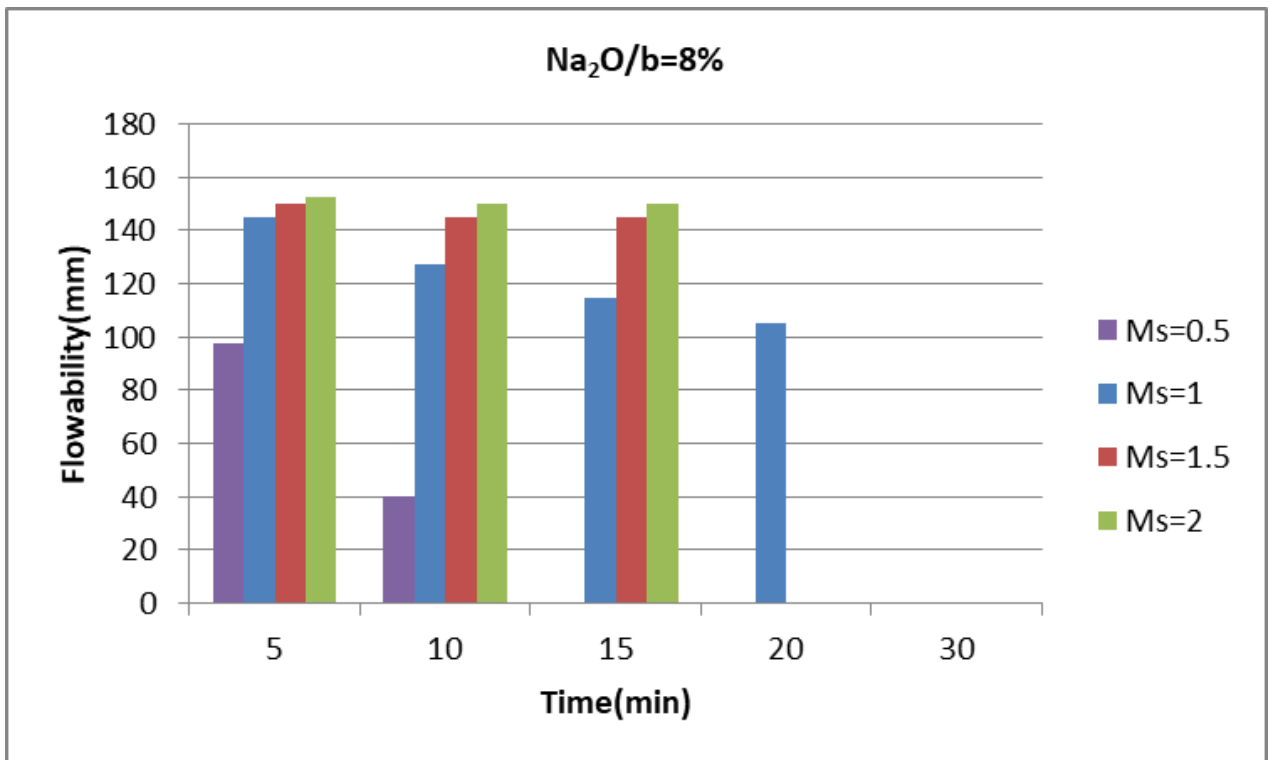
Fig. 5.5 depicts the influence of Ms ratio on slump retention of BFS-FA AAP of BFS/b ratio 0.5 and w/s ratio 0.4 for a constant Na<sub>2</sub>O/b ratio. In general, flowability of AAP decreases with time. At lower Ms ratio, the flowability decreased at a higher rate. Higher Ms ratio resulted in increase in flowability due to the decrease in the friction between particles due to more activator content. At higher Ms ratio, the flowability however decreased at lower rate but was retained only for 15 min. This may be due to faster reaction rates produced by higher concentration of SiO<sub>2</sub>.



(a)



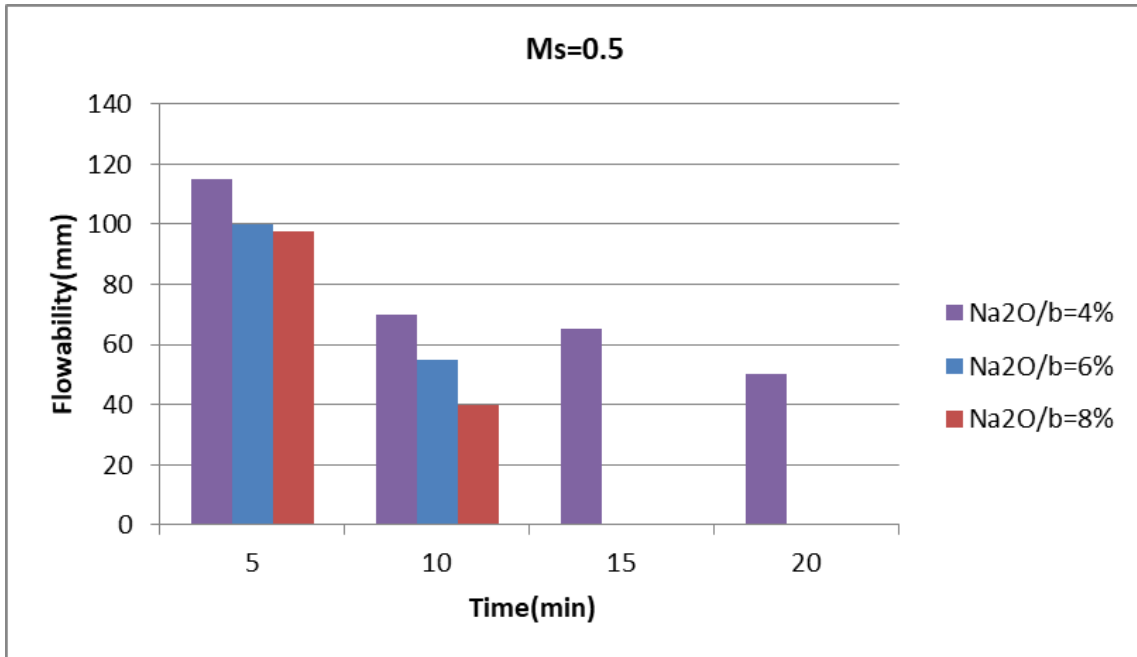
(b)



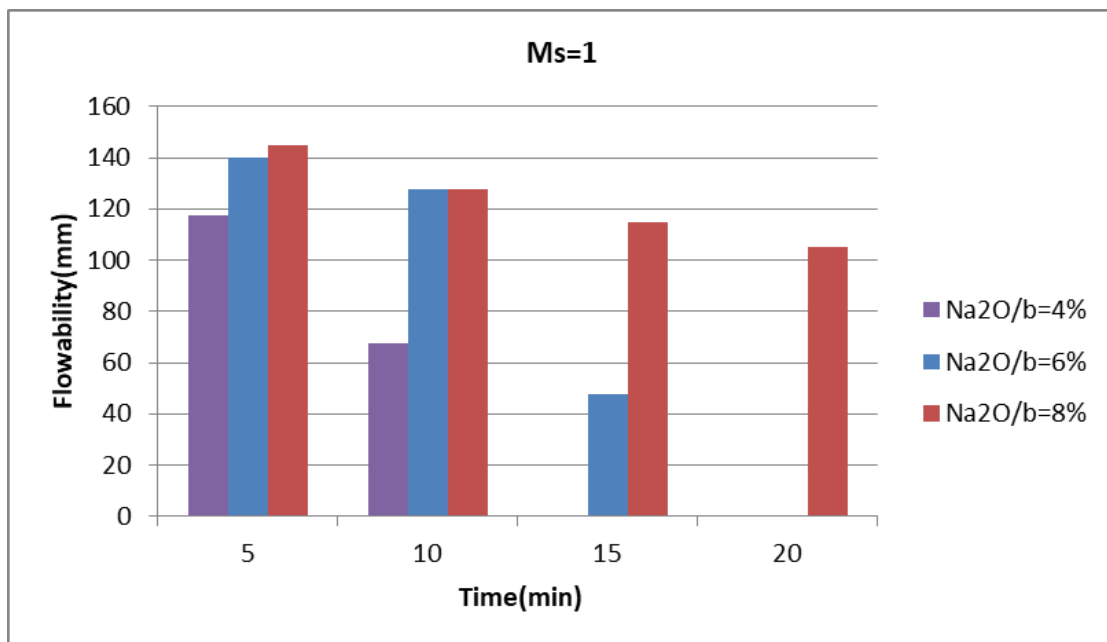
(c)

Fig. 5.5: Effect of Ms ratio on flowability of GGBS-FA AAB for (a) Na<sub>2</sub>O/b=4% (b) Na<sub>2</sub>O/b=6% (c) Na<sub>2</sub>O/b=8%

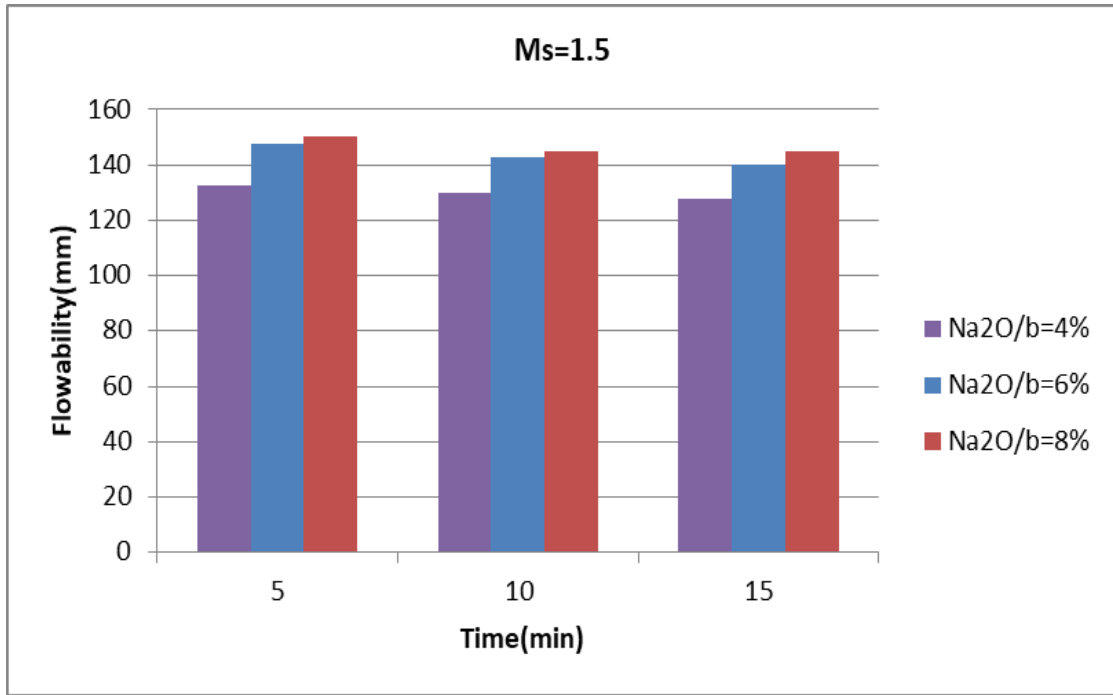
The influence of  $\text{Na}_2\text{O}/b$  ratio on the slump retention of BFS-FA AAP of BFS/ $b$  ratio 0.5 and  $w/s$  ratio 0.4 at a constant  $M_s$  ratio is shown in Fig. 5.6. At higher  $\text{Na}_2\text{O}/b$  ratio, the flowability was decreased at a higher rate. As  $\text{Na}_2\text{O}/b$  ratio and  $M_s$  ratio increases, the flowability reduction rate became gradual but flowability becomes zero after 15 mins. This can be due to the faster formation of reaction products due to high concentration of  $\text{OH}^-$  ions. At higher  $\text{Na}_2\text{O}/b$  ratio, more ions may be released and are absorbed by Si ions. Hence the flowability is reduced to zero quickly as the polycondensation of reaction products increases.



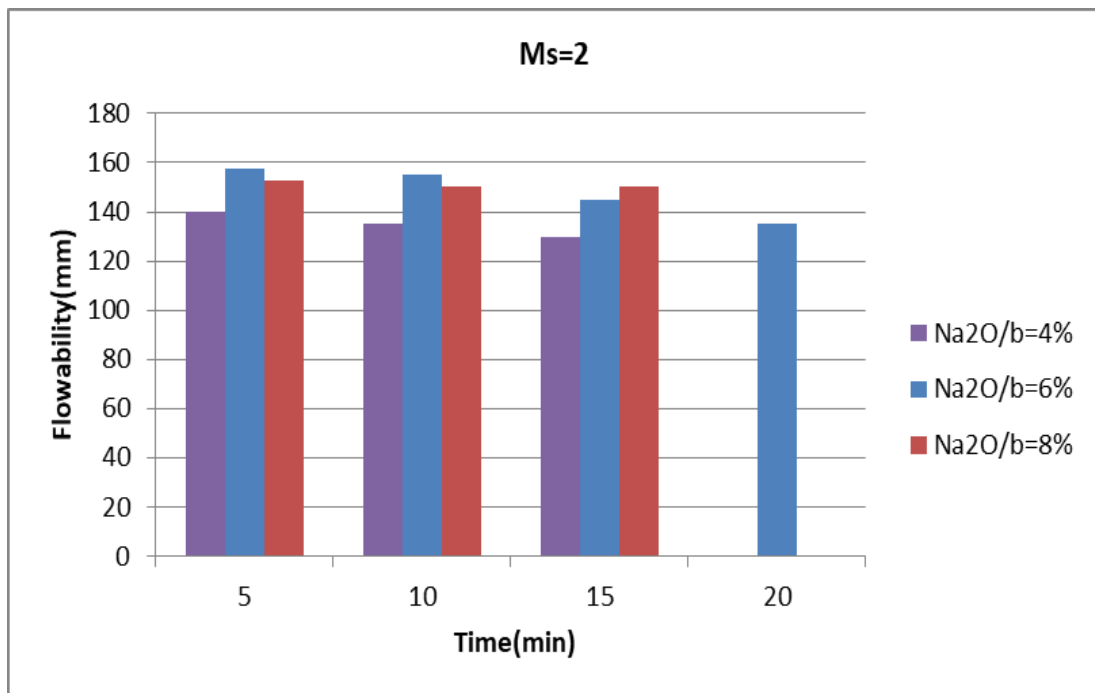
(a)



(b)



(c)



(d)

Fig. 5.6: Effect of Na<sub>2</sub>O/b ratio on flowability of GGBS-FA AAB for (a) Ms=0.5 (b) Ms=1 (c) Ms=1.5 (d) Ms=2

#### **5.1.4 INFERENCE**

At the end of phase 1 of the study it could be seen that both  $\text{Na}_2\text{O}/b$  ratio and  $M_s$  ratio are critical factors that affect the rheology of AAP. The setting time was found to decrease with increase in  $M_s$  ratio upto 1.5 and then increased. The mix with  $M_s$  ratio 1.5 exhibit gradual development of penetration resistance with a favorable setting time frame during which the paste remains workable. The setting time was decreased with increase in  $\text{Na}_2\text{O}/b$  ratio. When the ratio is 4% setting time was longer with very slow development of penetration resistance. the setting became very quick with rapid development of penetration resistance when  $\text{Na}_2\text{O}/b$  ratio is 8%. An optimum setting was observed when the  $\text{Na}_2\text{O}/b$  ratio was 6% and the development of penetration resistance is relatively gradual. Considering the flowability of AAP, it increased when  $\text{Na}_2\text{O}/b$  ratio is increased from 4 to 6% and decreased when  $\text{Na}_2\text{O}/b$  ratio is increased from 6 to 8% with an optimum value at 6%. The flowability increased with increase of  $M_s$  ratio and found to be high when  $M_s$  was greater than 1.5. Thus by considering the setting and flow characteristics of AAP, the optimum values of the  $\text{Na}_2\text{O}/b$  ratio and  $M_s$  ratio are taken as 6% and 1.5 respectively.

### **5.2 EFFECT OF BFS/b RATIO**

The effect of BFS/b ratio on the rheology of AAP and mechanical properties of AAM is studied in the second phase of the study. The rheology of the AAB system was investigated by conducting test on setting time, penetration resistance, flowability and slump retention on AAP. The mechanical properties of the AAM was evaluated by flexural strength test, compressive strength test and ultrasonic pulse velocity (UPV) test.

#### **5.2.1 EFFECT ON SETTING TIME OF AAP**

Fig. 5.7 shows the influence of BFS/b ratio on the setting time of BFS-FA AAP with  $\text{Na}_2\text{O}/b$  ratio 6%,  $M_s$  ratio 1.5 and w/s ratio 0.4. It can be seen that as the BFS/b ratio increased, both final and initial setting time gets reduced. When the BFS/b ratio is 0, i.e. with 100% fly ash content, the paste didn't set even after 10 hours. However when slag was introduced into the mixture the setting time was reduced. It was observed that the final setting time of the AAP was reached within 5 hours when BFS/b ratio is 0.25. The setting time got further shorter when the slag content was increased. There is a huge reduction in the setting time when the BFS/ b ratio is increased from 0.25 to 0.50. The initial setting time decreased by 47% and final setting time decreased by 43%. The initial setting time was 47 min and final setting time

was 2.5 hours for BFS/b ratio 0.5. When the BFS/b ratio is increased to 0.75 and 1, the initial setting time was 32 min and 28 min respectively and the final setting of the AAP was 2.25 hours and 1.75 hours respectively.

The great variance in the setting time shows that the BFS/b ratio is an important control factor of setting time. When fly ash was only used as the binder, the setting time is too long. As the fly ash is replaced with slag the setting time became faster. This is explained by the high CaO level in the slag, which quickens the hydration reaction of the paste (Lee and Lee 2013). Hence fly ash need to be incorporated in the AAP to reach a reasonable setting time.

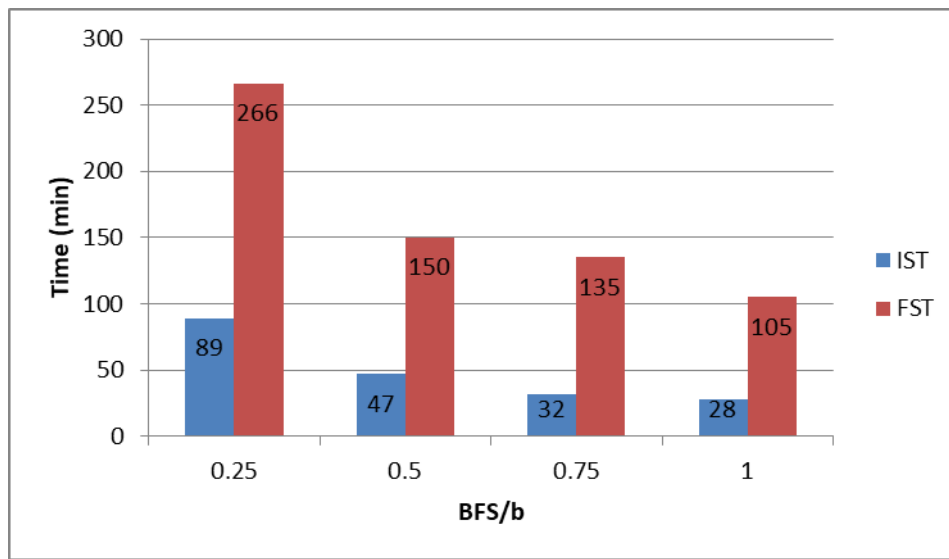


Fig. 5.7: Effect of BFS/b ratio on setting time of GGBS-FA AAP for  $M_s=1.5$  and  $Na_2O/b=6\%$

### 5.2.2 EFFECT ON PENETRATION RESISTANCE OF AAP

The effect of BFS/b ratio on the penetration resistance of BFS-FA AAP with  $Na_2O/b$  ratio 6%,  $M_s$  ratio 1.5 and w/s ratio 0.4 and its variation with time is shown in Fig. 5.8. When the BFS/b was 0, referring to binder with only fly ash, the paste exhibit zero penetration resistance. The vicat needle penetrated to the full depth even after 10 hours. The higher fly ash content leads to delayed formation of the reaction products as it has low calcium content. With the introduction of slag in to the binder of AAP the paste started to develop penetration resistance. It took more than an hour for the AAP with BFS/b ratio 0.25 to develop resistance and the curve has a gentle slope. The paste developed penetration resistance very slowly. For the BFS/b ratio 0.5, the slope of the curve was gradual. With increase in time, the penetration resistance increased uniformly. There was enough time frame within which the paste

remained workable. For BFS/b ratio 0.75 and above, the curve has a steep slope. After initial setting of the paste, the penetration resistance reached its maximum very quickly. The paste remained workable for short period only.

The variation in the penetration resistance curve shows that the BFS/b ratio is a dominant factor that affects the rheology of the AAP. The penetration resistance was increased when slag content is introduced in the system. The introduction of slag means faster dissolution and higher structure build-up rate which was characterized by increase in penetration resistance. These results are due to the formation of more early C-A-S-H gels (Lu et al. 2021). So both slag and fly ash need to be present in the AAP for it to show a better penetration resistance.

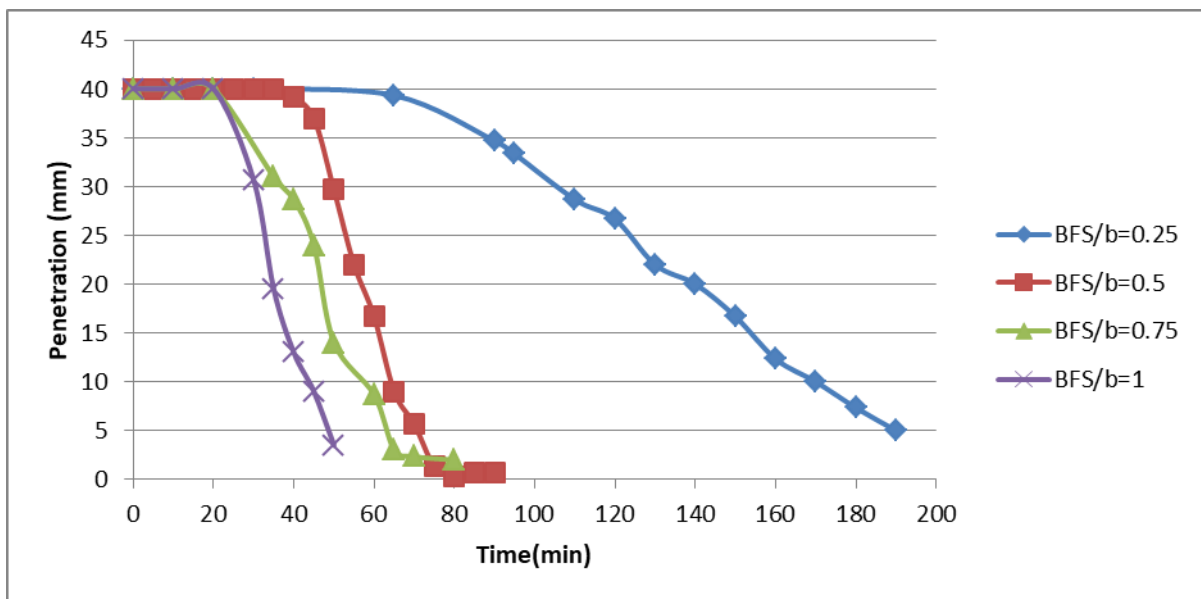


Fig. 5.8: Variation of penetration resistance with BFS/b ratio for  $M_s=1.5$  and  $Na_2O/b=6\%$

### 5.2.3 EFFECT ON FLOWABILITY AND SLUMP RETENTION OF AAP

The influence of BFS/b on the 5 mins flowability of BFS-FA AAP with  $Na_2O/b$  ratio 6%,  $M_s$  ratio 1.5 and w/s ratio 0.4 is shown in Fig. 5.9. For every 0.1 increase of BFS/b ratio the flowability reduce by 1.5 mm. Thus as the BFS/b ratio increases the flowability decreases. This may be due to the higher slag content for higher BFS/b ratio that leads to more irregular particles. This will in turn lead to increase of surface area and decrease of lubrication effect. Hence more water may be required to obtain the desirable workability.

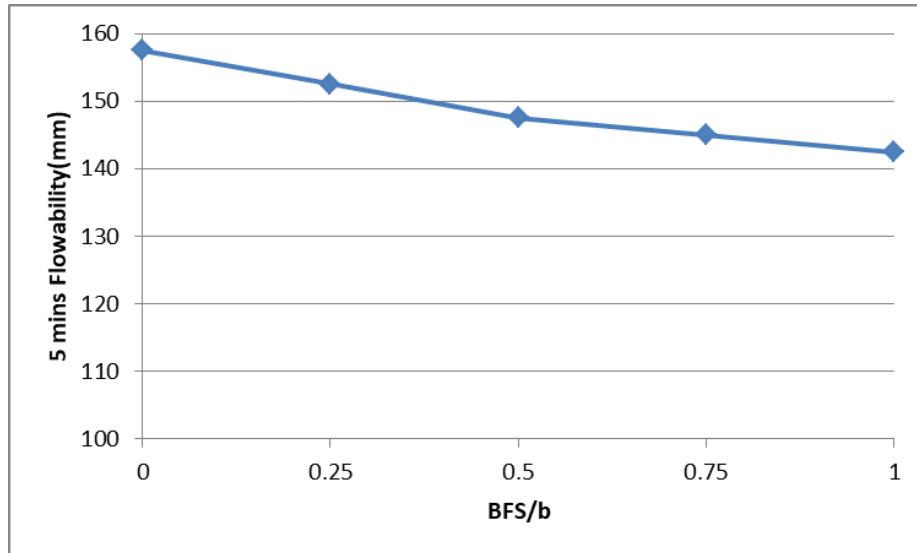


Fig. 5.9: Effect of BFS/b ratio on the flowability of GGBS-FA AAB

The influence of BFS/b on the slump retention of BFS-FA AAP with  $\text{Na}_2\text{O}/b$  ratio 6%, Ms ratio 1.5 and w/s ratio 0.4 is shown in Fig. 5.10. The flowability of BFS-FA AAP with BFS/b ratio of 0 and 0.25 declined very slowly. There was significant reduction in flowability overtime when BFS/b was increased to 0.5 and 0.75. When the BFS/b was 1 the flowability of the AAP drops dramatically and could not be tested after 15 min. Due to the differing reactivity of slag and fly ash at ambient temperature, there is a significant variance in flowability. In comparison to slag, fly ash has a relatively lower glassy phase content but a lower Ca content. The flowability of BFS-FA AAP with a higher BFS/b ratio thus tends to degrade more quickly over time as a result of substantially higher reaction rate.

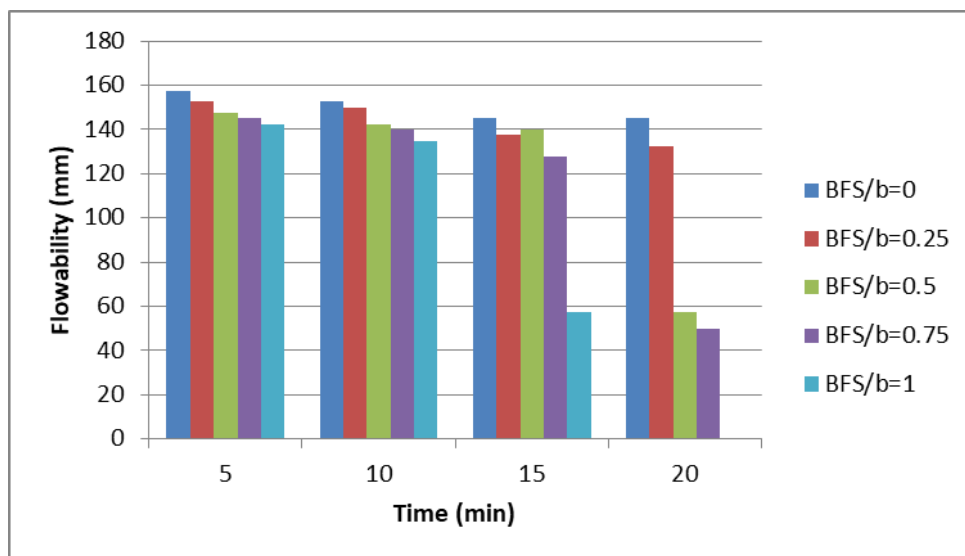


Fig. 5.10: Effect of BFS/b ratio on flowability of GGBS-FA AAB for Ms=1.5 and  $\text{Na}_2\text{O}/b=6\%$

### 5.2.4 EFFECT ON DENSITY OF AAM

Fig. 5.11 depicts the density of BFS-FA AAM with  $\text{Na}_2\text{O}/b$  ratio 6%,  $M_s$  ratio 1.5 and  $w/s$  ratio 0.4 at 7 and 28 days for different BFS/ $b$  ratio. As the BFS/ $b$  ratio increases the density increases. For BFS/ $b$  ratio of 0, the density of AAM specimen was  $1948 \text{ kg/m}^3$  at 7 days and  $1966.98 \text{ kg/m}^3$  at 28 days with an overall increase of 0.9%. The AAM specimen with only fly ash as the binder has the least density. The density of the mortar is found to increase with the addition of slag into the matrix. Lower densities of AAM at lower slag-fly ash ratio could be due to lesser specific gravity of fly ash (around 2.2) compared to slag (around 2.9). There is drastic change in the density when the BFS/ $b$  ratio changed from 0.25 to 0.5 by about 10%. The density of AAM with BFS/ $b$  ratio of 1 was  $2338 \text{ kg/m}^3$  at 7 days and  $2354 \text{ kg/m}^3$  at 28 days with an overall increase of 0.7%. The variation of density between the 7 and 28 days is due to the formation of polymerization products overtime. The density of the specimen was increased by around 20%, when the BFS/ $b$  ratio increased from 0 to 1. This is due to variation in the formation of reaction products for slag and fly ash at the ambient curing condition. Fly ash having less Ca content has less reactivity under ambient condition. However slag has more Ca content hence highly reactive even under ambient condition. This formation of the polymerization products thus lead to a much denser mix. Thus slag needs to be incorporated into the mix for the BFS-FA AAM to be denser.

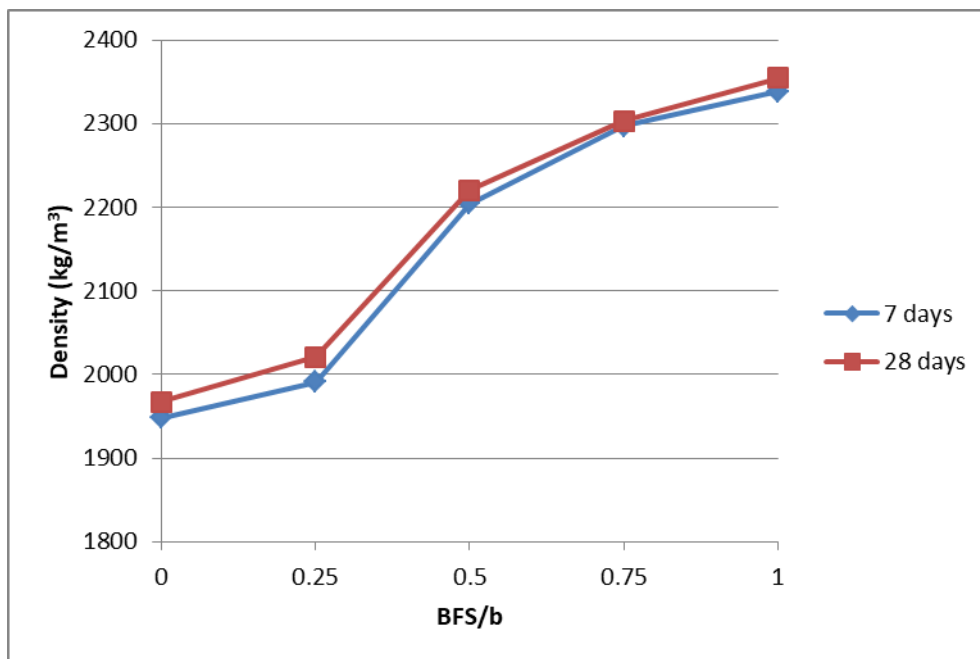


Fig. 5.11: Variation of density of AAM specimens with BFS/ $b$  ratio

### 5.2.5 EFFECT ON UPV OF AAM

Fig. 5.12 shows the effect of BFS/b ratio on the ultrasonic pulse velocity through BFS-FA AAM with  $\text{Na}_2\text{O}/b$  ratio 6%, Ms ratio 1.5 and w/s ratio 0.4 at 7 and 28 days. At zero slag content the velocity obtained is very low, 603 m/s at 7 days and 1382 m/s at 28 days indicating a non-homogeneous mix with voids. The velocity through the mortar specimen is found to increase with the increase in the BFS/b ratio. The velocity increases rapidly at BFS/b ratio of 0.25 due to addition of slag into the AAM, 2702 m/s at 7 days and 2891 m/s at 28 days. The shift in the velocity between 7 and 28 days is due to the formation of reaction products overtime leading to a uniform structure.

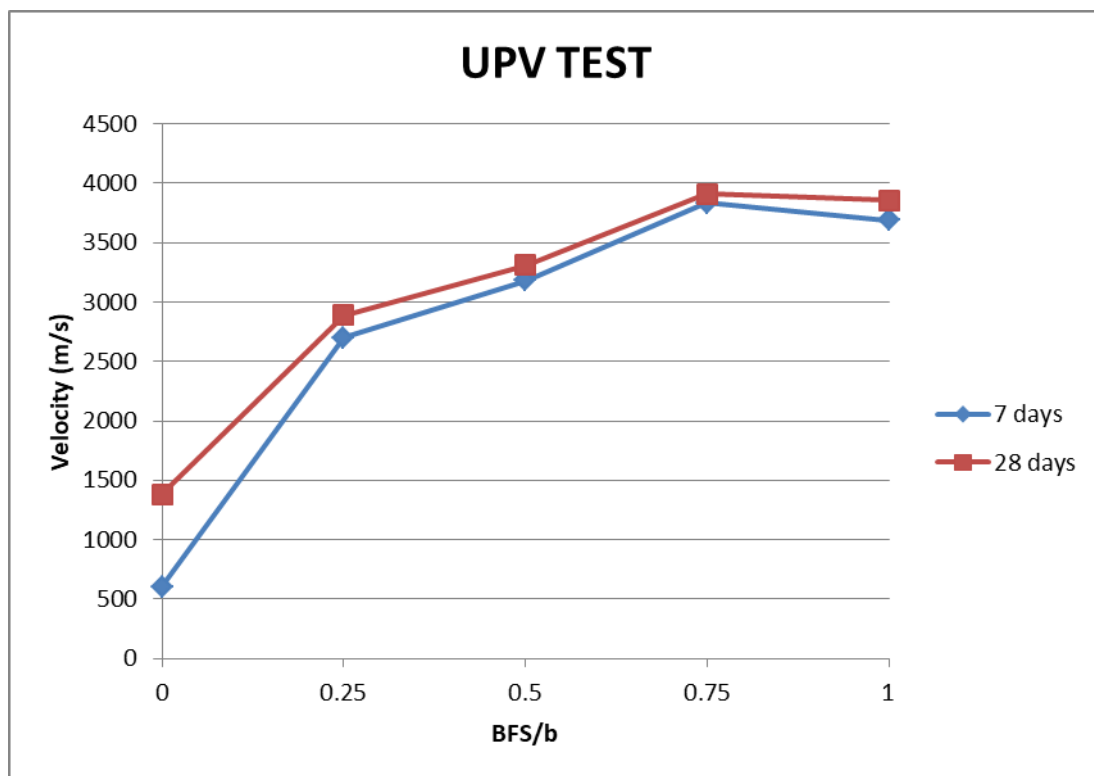


Fig. 5.12: Effect of BFS/b on UPV of AAM

### 5.2.6 EFFECT ON COMPRESSIVE STRENGTH OF AAM

The effect of BFS/b ratio on the compressive strength of BFS-FA AAM with  $\text{Na}_2\text{O}/b$  ratio 6%, Ms ratio 1.5 and w/s ratio 0.4 at 7 and 28 days is depicted in Fig. 5.13. The compressive strength of the AAM specimen was increased with the increase in the BFS/b ratio. For BFS/b ratio of 0, the compressive strength of the sample was 0 MPa at 7 days which can be attributed to less reactivity of the fly ash at the ambient condition. The strength however

increased to 7.1 MPa at 28 days due to formation of reaction product overtime. When the 25% of the fly ash was replaced by slag, the compressive strength increased to 3.8 MPa at 7 days and 12.1 MPa at 28 days. Relatively high compressive strength was developed when the BFS/b ratio was increased to 0.5 and above. The 28 days compressive strength of AAM sample of BFS/b ratio 0.5, 0.75 and 1 was observed to be 50 MPa, 69.1 MPa and 71.7 MPa respectively. The variation of the compressive strength with BFS/b was not linear. Thus, it can be said that the two precursors function jointly rather than individually in influencing compressive strength to some extent.

The BFS/b ratio is an important variable that affects compressive strength since it significantly influenced the composition and structure of the reaction product. The ratios of Ca/Si and Si/Al steadily rise when the BFS/b ratio rises, producing more CASH gel and less NASH gel together. The coexistence of NASH and CASH type gels in the mix blend was responsible for the rise in compressive strength with increased BFS in the mix blend, which can lead to a denser and more uniform matrix and, eventually, improved mechanical characteristics. A more uniform and compacted structure is created as a result of increased degree of cross-linking of reaction products (Rafeet et al. 2019). The variation of the compressive strength between 7 and 28 days can be attributed to formation of more NASH type gel and CASH type gel in the due course.

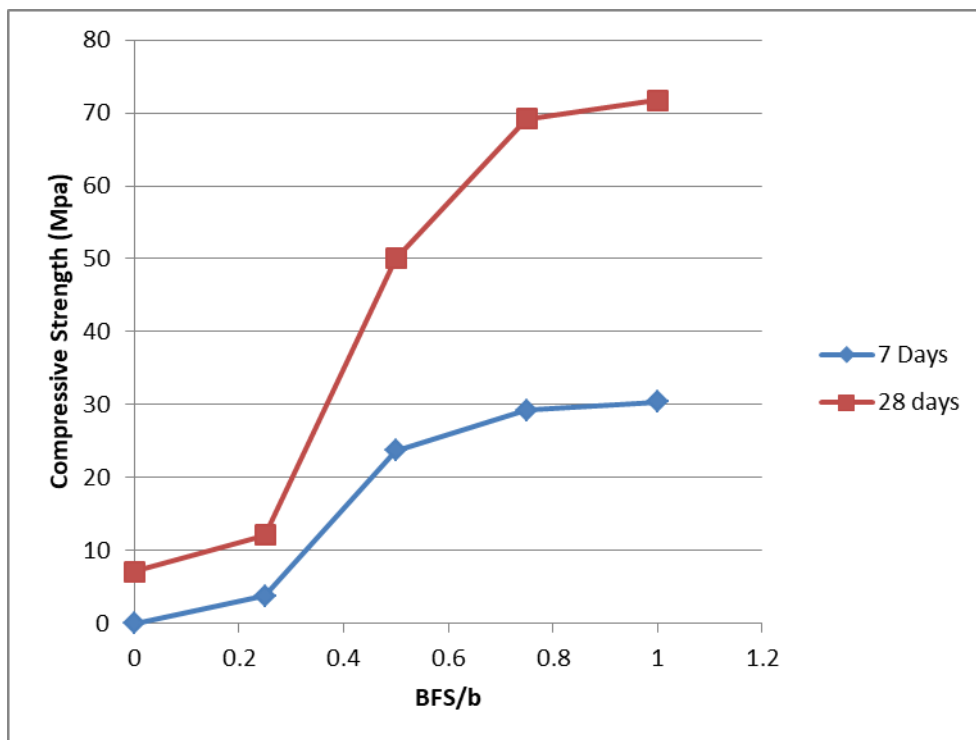


Fig. 5.13: Effect of BFS/b on compressive strength of AAM

### 5.2.6 EFFECT ON FLEXURAL STRENGTH OF AAM

The effect of BFS/b ratio on the flexural strength of BFS-FA AAM with  $\text{Na}_2\text{O}/\text{b}$  ratio 6%,  $\text{Ms}$  ratio 1.5 and  $\text{w/s}$  ratio 0.4 at 7 and 28 days is depicted in Fig. 5.14. The effect of BFS/b ratio on flexural strength is similar to that of compressive strength. The AAM prisms of BFS/b ratio of 0 had no flexural strength. This may be due to less reactivity of fly ash at the ambient curing condition. As slag is incorporated into the binder the flexural strength increases. When the BFS/b ratio was increase to 0.25, the AAM specimen developed flexural strength of 2.7 MPa at 7 days and 2.9 MPa at 28 days. The 28 day flexural strength of AAM specimen of BFS/b ratio 0.5, 0.75 and 1 are 8.3 MPa, 11.1 MPa, and 10.3 MPa respectively. Flexural strength was observed to be approximately 1/6 of the compressive strength. Here also the increase in the flexural strength with the BFS/b ratio was due to the formation of CASH type and NASH type gel that result in the formation a compacted structure.

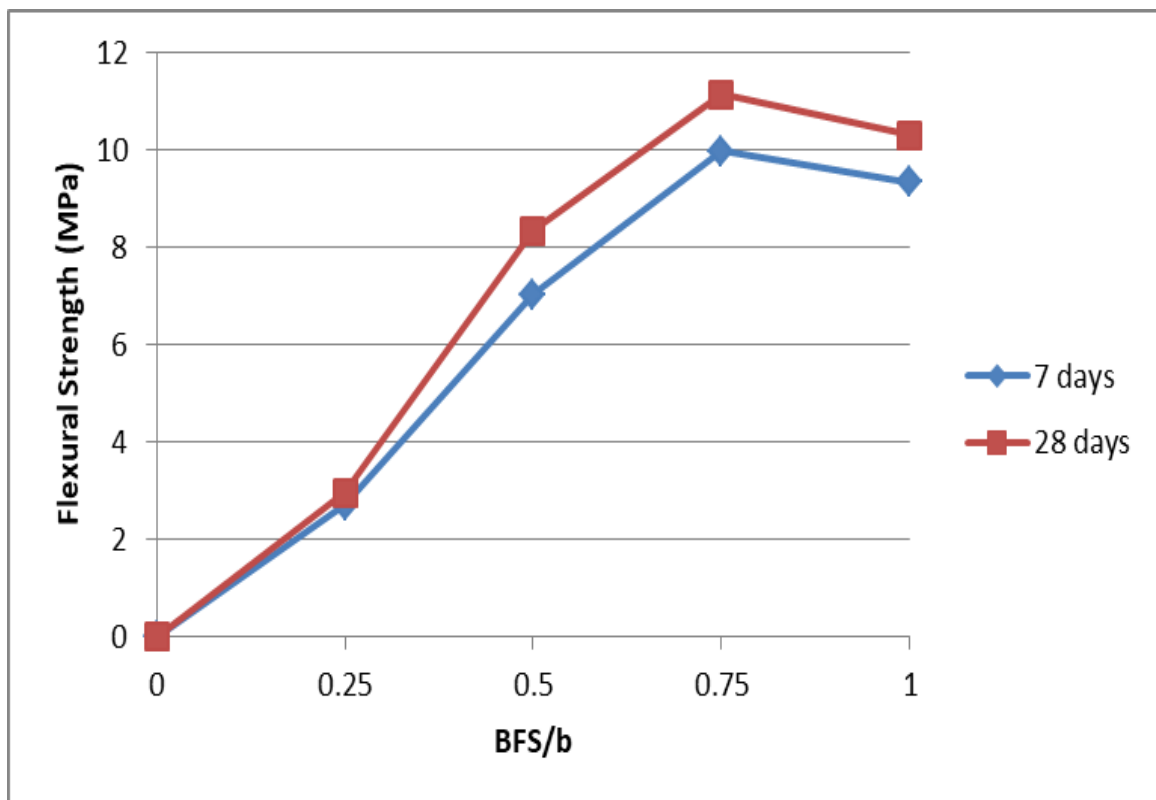


Fig. 5.14: Effect of BFS/b on flexural strength of AAM

### **5.2.7 INFERENCE**

At the end of phase 2 of the study, it was observed that BFS/b ratio has noteworthy effect on both the rheology and mechanical properties. The addition of a certain proportion of fly ash into the binder will not greatly impact the strength, but it provides the benefits of retarding setting time and increasing the flowability of BFS-FA AAB system. With this consideration, a reasonably designed BFS/FA ratio of BFS/FA AAB system is crucial for the application. A reasonable strength of the AAM was observed for BFS/b ratio of 0.5 and above. The AAM also had a denser and homogenous structure for BFS/b ratio 0.5 and above. The initial setting time of the AAP was observed to be less than 30 min at BFS/b ratio of 1. A reasonable initial setting time was obtained for BFS/b ratio 0.5 and 0.75 (47 min and 32 min respectively). The AAP also developed penetration resistance within short time period at higher BFS/b ratio. The flowability of AAP was also reduced at high BFS/b ratio. Hence by considering both the rheology and mechanical properties, the BFS/b ratio 0.5 and 0.75 are used for the next phase of the study

### **5.3 EFFECT OF ADMIXTURES**

The phase 3 of the study deals with the effect of admixtures namely phosphoric acid and red gypsum on the rheology of the BFS-FA AAP. The optimum values of the control factors obtained from phase 1 and 2 of the study is used in this phase. BFS-FA AAP with various combination mixes of red gypsum and phosphoric acid as mentioned in Table 3.7 are tested to study its effect on the setting time. The flowability of the AAP is also evaluated in each case and compared to AAB without admixture.

In the first step, red gypsum and phosphoric acid were added together, as mentioned in mix 1 in Table 3.7, into BFS-FA AAP with  $\text{Na}_2\text{O}/b$  ratio 6%, Ms ratio 1.5, w/s ratio 0.4 and BFS/b ratio 0.5 and tested for setting time. The red gypsum were taken as 2.5%, 5%, 7.5%, 10% of the binder content. The phosphoric acid of 0.8M is used. Fig. 5.15 shows the setting time test of AAP with 0.8M phosphoric acid and red gypsum at 2.5% and 5%. At all the different combination of admixtures used, the setting time of AAP was retarded for more than 24 hours.



(a)



(b)

Fig. 5.15 Setting time test on AAP with 0.8M phosphoric acid and red gypsum at (a) 2.5% and (b) 5% of binder content

As the setting time was retarded to a great extent in the first case, the red gypsum of 2.5% of binder content and 0.8M  $H_3PO_4$  was added to AAP with higher BFS/b ratio of 1 without varying other control factors in the second step as mentioned in mix 2 of Table 3.7. From the phase 2 of the study it was observed that with slag as the only binder, the AAP sets quickly with an IST of 28 minutes. However when the admixtures were added in the proportion mentioned above, the setting of the AAP was retarded to more than 24 hours. Hence it was figured that the admixtures added have high retarding effect at the mentioned proportions and combinations even at high slag content.



Fig. 5.16: Setting time test on AAP of 100% slag with 0.8M phosphoric acid and red gypsum at 2.5% of binder content

The effect of the phosphoric acid alone as admixture on the setting time was studied in the third step of this phase. Phosphoric acid solution of molarity 0.5 and 0.8 was added to the BFS-FA AAP of  $\text{Na}_2\text{O}/b$  ratio 6%, Ms ratio 1.5, w/s ratio 0.4 and BFS/b ratio 0.5 as mentioned as mix 3 in Table 3.7. The setting time was retarded at both of the molarity used. At 0.8M the AAP didn't set even after 24 hours. Thus the retarding effect of phosphoric acid was concluded at this stage. It was observed that increasing the phosphoric acid concentration retarded the setting time. After the phosphoric acid concentration increased from 0.5M to 0.8M, a dramatic increase in the setting time can be found. This implies that the setting time is very sensitive to the phosphoric acid concentration. When 0.8M phosphoric acid is used as a retarder, the setting time exceeded 24 hours, which is too long in engineering practice. Thus a molarity of 0.5 and lower may be used for further stages of the study.



Fig. 5.17: Setting time test on AAP with 0.8M phosphoric acid as admixture

In the fourth stage, the effect of red gypsum alone as admixture on the setting time of BFS-FA AAP of  $\text{Na}_2\text{O}/b$  ratio 6%,  $M_s$  ratio 1.5,  $w/s$  ratio 0.4 and BFS/ $b$  ratio 0.5, as mentioned in mix 4 of Table 3.7, was studied. From the phase 2 of the study it was observed that AAP with BFS/ $b$  ratio 0.5 has a IST of 47 min and a FST of 150 min. Fig. 5.18 shows the effect of various concentration of red gypsum on the setting time of AAP. Initially red gypsum was added at 2.5% of binder content and the setting was accelerated, with an IST of 26 min and FST of 115 min. When the quantity of red gypsum was reduced to 1%, the setting time was increased with an IST of 45 min and FST of 125 min which is almost equal to the setting time of AAP without admixtures. Even at low quantity of red gypsum setting time of AAP was accelerated by a small amount. As the quantity of red gypsum increases its accelerating property was enhanced. Thus red gypsum acted as an accelerator.

Even though gypsum ( $\text{CaSO}_4$ ) is used as a retarder in conventional cement concrete, it behaved differently in the AAB system. Setting time was reduced with the addition of red gypsum which has high quantity of  $\text{CaSO}_4$  (about 69%) and remaining quantity of iron hydroxide ( $\text{Fe}(\text{OH})_2$ ). The reduction in setting time can be attributed to the additional calcium ions entering the system when red gypsum was used. Thus a higher concentration of red gypsum resulted in a higher generation rate of CASH gel. Consequently, a faster setting was observed when the gypsum was added (Chang et al. 2005).

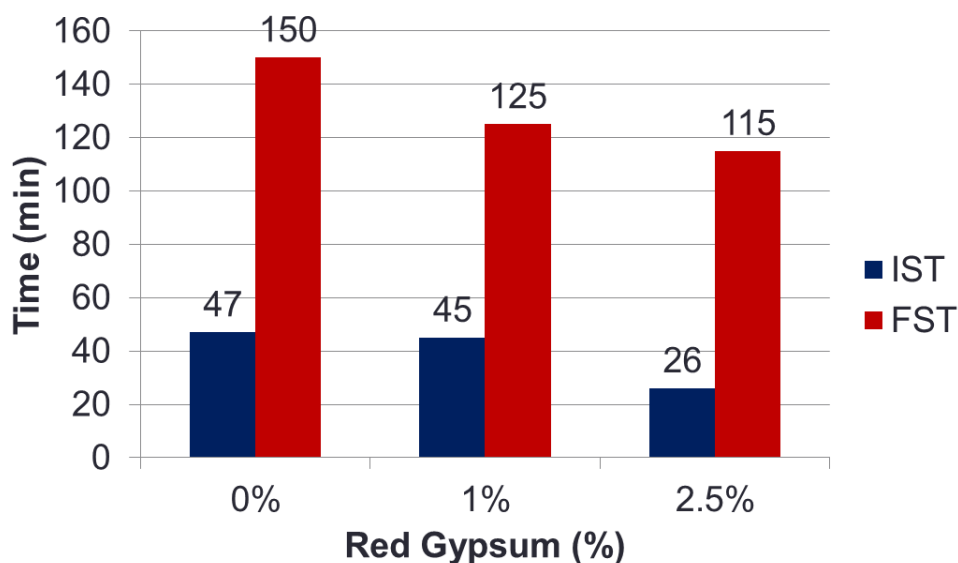


Fig. 5.18: Effect of red gypsum on setting time of BFS-FA AAP

From the previous steps it was observed that addition of 2.5% red gypsum accelerated the initial setting time by 21 minutes and phosphoric acid at 0.5M has retarded the setting time to more than 24 hours. Thus in the next stage red gypsum and phosphoric acid are added together as mentioned in mix 5, to achieve a reasonable setting time for the BFS-FA AAP. Red gypsum is added at 2.5% of the binder content. The molarity of phosphoric acid used includes 0.25M and 0.5M. Fig. 5.19 shows the setting time test on AAP with 0.5M phosphoric acid and red gypsum at 2.5%. When 2.5% red gypsum and 0.25M phosphoric acid was added to BFS-FA AAP of  $\text{Na}_2\text{O}/b$  ratio 6%, Ms ratio 1.5, w/s ratio 0.4 and BFS/b ratio 0.5, the IST was accelerated to 38 min and FST to 110 min. When 2.5% red gypsum and 0.5M phosphoric acid was added to BFS-FA AAP the setting time was however retarded. The AAP took more than 12 hours to set which is less than the time of setting when only 0.5M phosphoric acid was added as admixture. It is thus concluded red gypsum and phosphoric acid act in combination counteracting the accelerating and retarding property respectively. Thus it can be concluded that at 2.5% red gypsum content and a molarity of phosphoric acid between 0.25 and 0.5, a reasonable setting time of BFS-FA AAP can be achieved.



Fig. 5.19: Setting time test on AAP with 0.5M phosphoric acid and red gypsum at 2.5%

In the last step of this phase, the molarity of phosphoric acid at which the BFS-FA AAP has a reasonable setting time in the presence of 2.5% red gypsum is found. Two different molarity, 0.35M and 0.45M, are considered in between 0.25M -0.5M as obtained from previous step. The BFS/b ratio of 0.5 and 0.75 is used keeping other control factors same and the setting time is studied. The results are tabulated as shown in table 5.1. Fig. 5.20 shows the variation in setting time of BFS-FA AAP with BFS/b ratio of 0.5 for the various combination of admixture used. When 0.35M phosphoric acid and 2.5% red gypsum was used as admixture, the IST was accelerated by 6 min and FST by 20 min compared to AAP without any admixtures. When the molarity of phosphoric acid was increased to 0.45, the IST was retarded by 53 min and FST by 77 min. Thus 0.45M phosphoric acid and red gypsum at 2.5% binder content effectively retarded the setting time of BFS-FA AAP of  $\text{Na}_2\text{O}/\text{b}$  ratio 6%, Ms ratio 1.5, w/s ratio 0.4 and BFS/b ratio 0.5.

Table 5.1 IST and FST of BFS-FA AAP with various combinations of admixtures

Sl No	Molarity of phosphoric acid solution (M)	Quantity of red gypsum (%)	BFS/b	IST (min)	FST (min)
1	0	0	0.5	47	150
2	0.25	2.5	0.5	38	110
2	0.35	2.5	0.5	41	120
3	0.45	2.5	0.5	100	227
4	0	0	0.75	32	135
5	0.35	2.5	0.75	35	125
6	0.45	2.5	0.75	80	152

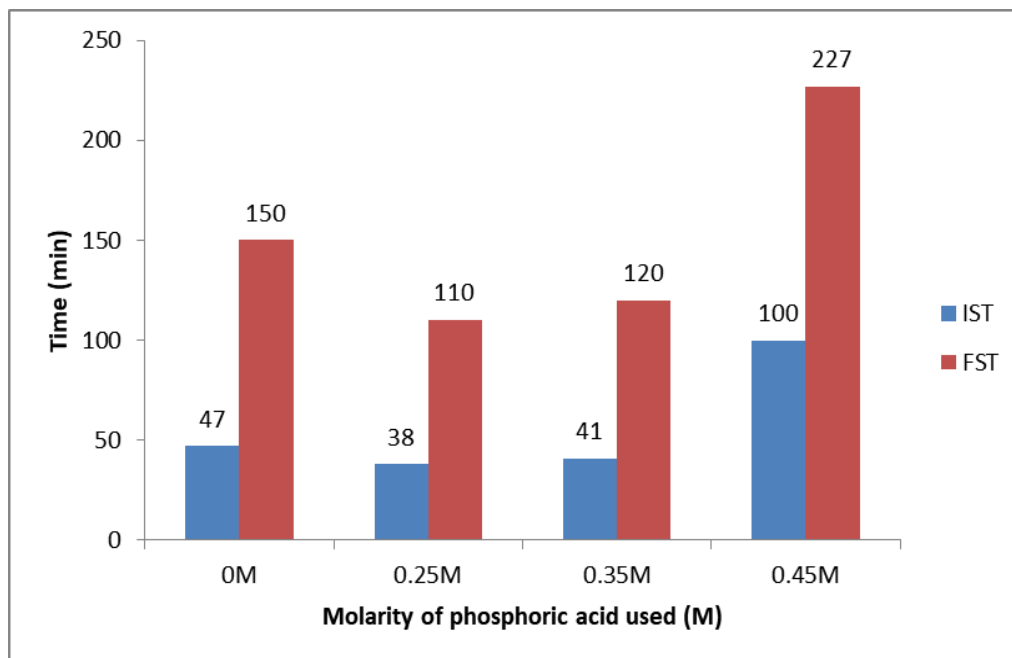


Fig. 5.20 Variation of setting time with the molarity of phosphoric acid for BFS-FA AAP of BFS/b ratio 0.5 and red gypsum of 2.5%

Fig. 5.21 shows the variation in setting time of BFS-FA AAP with BFS/b ratio of 0.75 for the various combination of admixture used. When 0.35M phosphoric acid and 2.5% red gypsum was used as admixture, the IST was retarded by 3 min and FST was accelerated by 10 min compared to AAP without any admixtures. When the molarity of phosphoric acid was increased to 0.45, the IST was retarded by 48 min and FST by 18 min. Thus 0.45M

phosphoric acid and red gypsum at 2.5% binder content effectively retarded the setting time of BFS-FA AAP of Na<sub>2</sub>O/b ratio 6%, Ms ratio 1.5, w/s ratio 0.4 and BFS/b ratio 0.5.

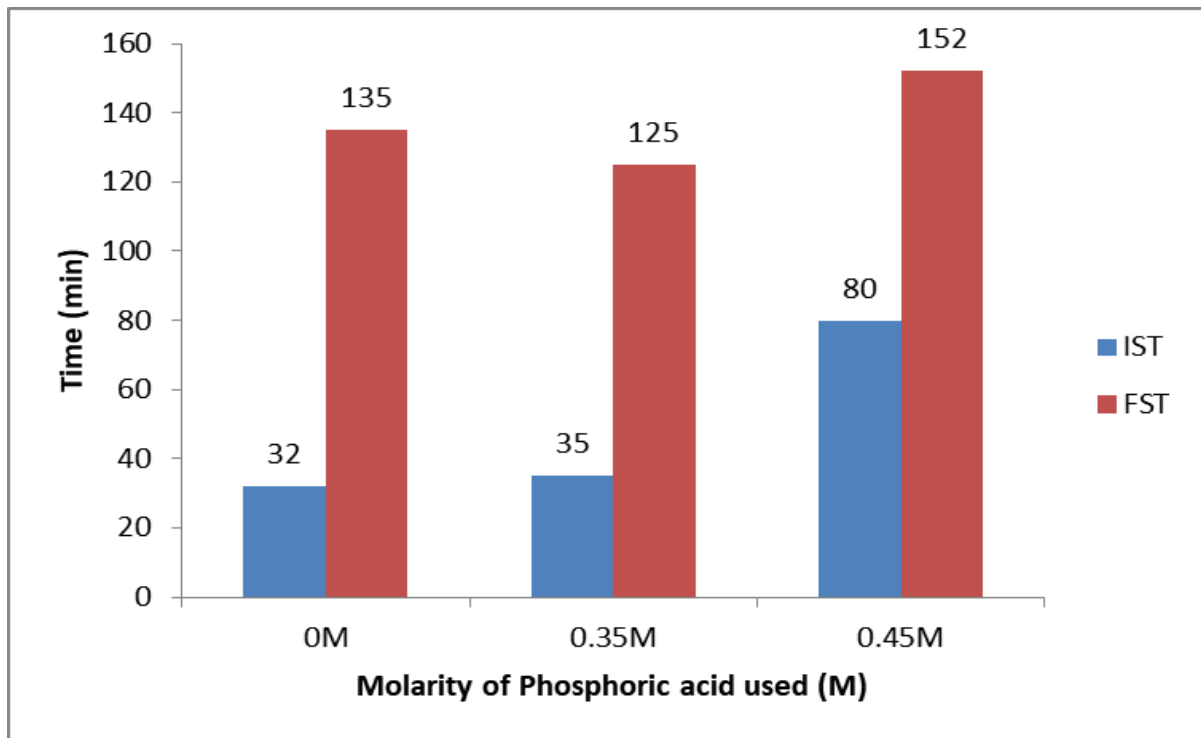


Fig. 5.21 Variation of setting time with the molarity of phosphoric acid for BFS-FA AAP of BFS/b ratio 0.75 and red gypsum of 2.5%

It was observed that adding red gypsum and phosphoric acid together blocked the retarding effect of the phosphoric acid. Despite the fact that the retarding effect on setting time was minimised, the setting time was still longer than the AAP without the phosphoric acid and red gypsum. This may be because the concentration of calcium ions increased when gypsum was mixed with phosphoric acid. As a result, the present concentration of phosphoric acid is insufficient to continue offering the same retarding impact. The retarding mechanism of phosphate acid is due to the formation of calcium phosphate. Due to the red gypsum, the solution included more calcium ions, so a larger concentration of phosphoric acid was needed to achieve the same retarding effect. This means that there are still excess calcium ions available for consumption by the hydration reaction of CSH gel, which shortens the setting time. Thus, a desirable setting time in AAP was reported at 0.45M phosphoric acid and 2.5% red gypsum concentration.

### **5.3.1 INFERENCE**

At the end of phase 3 of the study, the quantity of red gypsum and phosphoric acid required for effective retardation of the setting time was obtained. The phosphoric acid is retarder and heavily retarded the setting time when added as the only admixture in AAP. Red gypsum acted as an accelerator when added alone in AAP but when in added in combination with phosphoric acid of certain molarity the setting time of AAP can be retarded. The combination of red gypsum at 2.5% of binder content and 0.45M phosphoric acid yielded a favorable setting time for BFS-FA AAP with BFS/b ratio of 0.5 and 0.75. An IST of 100 min and FST of 227 min were obtained for BFS-FA AAP of BFS/b ratio 0.5 after the addition of admixture at the above mentioned quantity. The BFS/b ratio 0.75 the IST was 80 min and FST was 152 min with the addition of admixtures. Thus red gypsum and phosphoric acid can be used together to effectively retard the setting time of AAP.

## CHAPTER 6

### CONCLUSION

The Alkali Activated Slag-fly ash binder systems have many applications in the construction industry as they are an ecofriendly substitute to the cement based binders. The literature review shows that AABs have very low workability and setting time. The properties of AAB system depend on many factors like the  $\text{Na}_2\text{O}/\text{binder}$  ratio, the  $\text{SiO}_2/\text{Na}_2\text{O}$  ratio, the water/solid ratio, and the BFS/binder ratio. The rheology of the AABs must be properly understood to improve their setting time and workability. The effect control factors on the rheology and strength of the BFS-FA alkali activated binder system is studied and their values are optimized for further analysis. Red gypsum and phosphoric acid are used as admixture to modify the rheology of the binder by studying the setting behaviour of AAP.

From this study, it could be seen that  $\text{Na}_2\text{O}/\text{b}$  ratio and Ms ratio are critical factors that affect the rheology of AAP. A higher Ms ratio lead to higher workability. The setting time was found to decrease with increase in Ms ratio then increased. The mix with Ms ratio 1.5 exhibit gradual development of penetration resistance with a favorable setting time frame during which the paste remains workable. The flowability increased with increase of Ms ratio and found to be high when Ms was greater than 1.5. The setting time was decreased with increase in  $\text{Na}_2\text{O}/\text{b}$  ratio. An optimum setting was observed when the  $\text{Na}_2\text{O}/\text{b}$  ratio was 6% and the development of penetration resistance is relatively gradual. Considering the flowability of AAP, it increased when  $\text{Na}_2\text{O}/\text{b}$  ratio is increased and then decreased with an optimum value at 6%. Thus by considering the setting and flow characteristics, the optimum values of the  $\text{Na}_2\text{O}/\text{b}$  ratio and Ms ratio are taken as 6% and 1.5 respectively for the BFS-FA AAB system.

The effect of BFS/b ratio on both the rheology and mechanical properties are also studied. The addition of fly ash into the binder was found to have no significant impact on the strength of BFS-FA AAM at the ambient curing condition. However it provided the benefit of retarding setting time and increasing the flowability of the AAB system. A reasonable strength of the AAM was observed for BFS/b ratio of 0.5 and above. The AAM also had a denser and homogenous structure for BFS/b ratio 0.5 and above. The initial setting time obtained was relatively better when the BFS/b ratio 0.5 and 0.75 (47 min and 32 min respectively). The AAP also developed penetration resistance within short time period at higher BFS/b ratio. The flowability of AAP was also reduced at high BFS/b ratio. Hence by

considering both the rheology and mechanical properties, the BFS/b ratio 0.5 and 0.75 are used for the study of effect of admixtures on AAP.

In this study, effects of red gypsum and phosphoric acid on setting time of AAP were examined. The combined use of red gypsum and phosphoric acid was the main focus. It was concluded that using phosphoric acid alone increased the setting time. On the other hand, adding red gypsum alone reduced the setting time. The combined use of phosphoric acid and gypsum blocked the retarding effect of phosphoric acid. The phosphoric acid when added at 0.45M and red gypsum at 2.5% of binder content retarded the setting time of AAP effectively. Thus with the addition of admixtures the BFS-FA AAB systems can be used for construction purposes as a replacement to conventional concrete.

## REFERENCES

1. Alonso, M. M., S. Gismera, M. T. Blanco, M. Lanzón, and F. Puertas. 2017. “Alkali-activated mortars: Workability and rheological behaviour.” *Constr. Build. Mater.*, 145: 576–587. Elsevier Ltd. <https://doi.org/10.1016/j.conbuildmat.2017.04.020>.
2. ASTM C348-02. 2002. “Standard Test Method for Flexural Strength of Hydraulic-Cement Mortars.” *ASTM Int.*, 04: 1–6.
3. ASTM C349. 2002. “Standard test method for compressive strength of hydraulic-cement mortars (Using portions of prisms broken in flexure).” *ASTM Int.*, 1–6.
4. Athira, V. S., A. Bahurudeen, M. Saljas, and K. Jayachandran. 2021. “Influence of different curing methods on mechanical and durability properties of alkali activated binders.” *Constr. Build. Mater.*, 299: 123963. Elsevier Ltd. <https://doi.org/10.1016/j.conbuildmat.2021.123963>.
5. Bocullo, V., L. Vitola, D. Vaiciukyniene, A. Kantautas, and D. Bajare. 2021. “The influence of the SiO<sub>2</sub>/Na<sub>2</sub>O ratio on the low calcium alkali activated binder based on fly ash.” *Mater. Chem. Phys.*, 258 (September 2020): 123846. Elsevier B.V. <https://doi.org/10.1016/j.matchemphys.2020.123846>.
6. Chang, J. J. 2003. “A study on the setting characteristics of sodium silicate-activated slag pastes.” *Cem. Concr. Res.*, 33 (7): 1005–1011. [https://doi.org/10.1016/S0008-8846\(02\)01096-7](https://doi.org/10.1016/S0008-8846(02)01096-7).
7. Chang, J. J., W. Yeih, and C. C. Hung. 2005. “Effects of gypsum and phosphoric acid on the properties of sodium silicate-based alkali-activated slag pastes.” *Cem. Concr. Compos.*, 27 (1): 85–91. <https://doi.org/10.1016/j.cemconcomp.2003.12.001>.
8. Dai, X., S. Aydın, M. Y. Yardımcı, K. Lesage, and G. de Schutter. 2020. “Influence of water to binder ratio on the rheology and structural Build-up of Alkali-Activated Slag/Fly ash mixtures.” *Constr. Build. Mater.*, 264: 120253. Elsevier Ltd. <https://doi.org/10.1016/j.conbuildmat.2020.120253>.
9. Dai, X., S. Aydın, M. Y. Yardımcı, K. Lesage, and G. De Schutter. 2022. “Rheology and microstructure of alkali-activated slag cements produced with silica fume activator.” *Cem. Concr. Compos.*, 125 (November 2020): 104303. Elsevier Ltd. <https://doi.org/10.1016/j.cemconcomp.2021.104303>.
10. Fahim, G., M. Ismail, N. Hafızah, and A. Khalid. 2018. “Compressive strength and microstructure of assorted wastes incorporated geopolymer mortars : Effect of solution molarity.” *Alexandria Eng. J.* Faculty of Engineering, Alexandria University.

<https://doi.org/10.1016/j.aej.2018.07.011>.

11. Gao, X., Q. L. Yu, and H. J. H. Brouwers. 2015. "Reaction kinetics, gel character and strength of ambient temperature cured alkali activated slag-fly ash blends." *Constr. Build. Mater.*, 80: 105–115. <https://doi.org/10.1016/j.conbuildmat.2015.01.065>.
12. IS 650:1991. 1991. "Indian Specification for Standard Sand for Testing of Cement." *Indian Stand.*, 1–11.
13. Kathirvel, P. 2015. "Effect of Kaolin Content and Alkaline Concentration on the Strength Development of Geopolymer Concrete." (September).
14. Lee, N. K., and H. K. Lee. 2013. "Setting and mechanical properties of alkali-activated fly ash/slag concrete manufactured at room temperature." *Constr. Build. Mater.*, 47: 1201–1209. Elsevier Ltd. <https://doi.org/10.1016/j.conbuildmat.2013.05.107>.
15. Lu, C., Z. Zhang, C. Shi, N. Li, D. Jiao, and Q. Yuan. 2021. "Rheology of alkali-activated materials: A review." *Cem. Concr. Compos.*, 121 (April): 104061. Elsevier Ltd. <https://doi.org/10.1016/j.cemconcomp.2021.104061>.
16. Mehta, A., R. Siddique, T. Ozbakkaloglu, F. Uddin Ahmed Shaikh, and R. Belarbi. 2020. "Fly ash and ground granulated blast furnace slag-based alkali-activated concrete: Mechanical, transport and microstructural properties." *Constr. Build. Mater.*, 257: 119548. Elsevier Ltd. <https://doi.org/10.1016/j.conbuildmat.2020.119548>.
17. Provis, J. L. 2018. "Cement and Concrete Research Alkali-activated materials." *Cem. Concr. Res.*, 114: 40–48. Elsevier Ltd. <https://doi.org/10.1016/j.cemconres.2017.02.009>.
18. Puertas, F., B. González-Fonteboa, I. González-Taboada, M. M. Alonso, M. Torres-Carrasco, G. Rojo, and F. Martínez-Abella. 2018. "Alkali-activated slag concrete: Fresh and hardened behaviour." *Cem. Concr. Compos.*, 85: 22–31. <https://doi.org/10.1016/j.cemconcomp.2017.10.003>.
19. Rafeet, A., R. Vinai, M. Soutsos, and W. Sha. 2019. "Effects of slag substitution on physical and mechanical properties of fly ash-based alkali activated binders (AABs)." *Cem. Concr. Res.*, 122 (June 2018): 118–135. Elsevier. <https://doi.org/10.1016/j.cemconres.2019.05.003>.
20. Rajamane, N. P., M. C. Nataraja, N. Lakshmanan, and P. S. Ambily. 2012. "Literature Survey on Geopolymer Concretes and A Research Plan in Indian Context." *The Masterbuilder*, (May): 50–56.
21. Serdar, M., A. Runci, Y. Guang, J. Provis, F. Dehn, T. Trintafillou, G. Habert, and S. Matthys. 2021. "Alkali activated materials – a new generation of cementless binders for concrete." *CPI – Concr. Plant Int.*, 2: 30–35.

22. Sun, B., Y. Sun, G. Ye, and G. De Schutter. 2022. "A mix design methodology of slag and fly ash-based alkali-activated paste." *Cem. Concr. Compos.*, 126 (November 2021): 104368. Elsevier Ltd. <https://doi.org/10.1016/j.cemconcomp.2021.104368>.
23. Tong, S., Z. Yuqi, and W. Qiang. 2021. "Recent advances in chemical admixtures for improving the workability of alkali-activated slag-based material systems." *Constr. Build. Mater.*, 272 (xxxx). <https://doi.org/10.1016/j.conbuildmat.2020.121647>.
24. Wang, D., Q. Wang, and Z. Huang. 2020. "New insights into the early reaction of NaOH-activated slag in the presence of CaSO<sub>4</sub>." *Compos. Part B Eng.*, 198: 108207. Elsevier Ltd. <https://doi.org/10.1016/j.compositesb.2020.108207>.

## APPENDIX I

Table i: Mix proportion of AAP for phase 1 experiments for 100g binder and w/s ratio of 0.4

Sl. No.	M <sub>s</sub>	Na <sub>2</sub> O/b (%)	Na <sub>2</sub> O(g)	SiO <sub>2</sub> (g)	Sodium Silicate solution (g)				12M Sodium Hydroxide solution (g)				Total (i.e. 12M solution)	Extra water (g or mL)	
					Solids			Total (i.e. solution)	Solids			Water			
					Na <sub>2</sub> O	SiO <sub>2</sub>	Total	Water	Total (i.e. solution)	Na <sub>2</sub> O	H <sub>2</sub> O	Total	Water		
1	0.00	4	4	0	0.00	0.00	0.00	0.00	0.00	4.00	1.16	5.16	9.14	14.30	31.30
2	0.00	6	6	0	0.00	0.00	0.00	0.00	0.00	6.00	1.74	7.74	13.70	21.45	26.95
3	0.00	8	8	0	0.00	0.00	0.00	0.00	0.00	8.00	2.32	10.32	18.27	28.59	22.61
4	0.50	4	4	2	0.83	2.00	2.83	1.93	4.76	3.17	0.92	4.09	7.23	11.32	32.32
5	0.50	6	6	3	1.25	3.00	4.25	2.89	7.14	4.75	1.38	6.13	10.85	16.98	28.48
6	0.50	8	8	4	1.67	4.00	5.67	3.86	9.52	6.33	1.84	8.17	14.47	22.64	24.64
7	1.00	4	4	4	1.67	4.00	5.67	3.86	9.52	2.33	0.68	3.01	5.33	8.34	33.34
8	1.00	6	6	6	2.50	6.00	8.50	5.79	14.29	3.50	1.02	4.52	7.99	12.51	30.00
9	1.00	8	8	8	3.33	8.00	11.33	7.71	19.05	4.67	1.35	6.02	10.66	16.68	26.67
10	1.50	4	4	6	2.50	6.00	8.50	5.79	14.29	1.50	0.44	1.94	3.43	5.36	34.35
11	1.50	6	6	9	3.75	9.00	12.75	8.68	21.43	2.25	0.65	2.90	5.14	8.04	31.53
12	1.50	8	8	12	5.00	12.00	17.00	11.57	28.57	3.00	0.87	3.87	6.85	10.72	28.71
13	2.00	4	4	8	3.33	8.00	11.33	7.71	19.05	0.67	0.19	0.86	1.52	2.38	35.37
14	2.00	6	6	12	5.00	12.00	17.00	11.57	28.57	1.00	0.29	1.29	2.28	3.57	33.05
15	2.00	8	8	16	6.67	16.00	22.67	15.43	38.10	1.33	0.39	1.72	3.05	4.77	30.74